Dear Editor,

We are pleased to submit our revised manuscript. The detailed comments by the three reviewers were very helpful to improve the quality of the current manuscript. Below we provide our point-by-point response to the three reviewers and a marked-up manuscript version showing the changes we made.

We are looking forward to your decision,

With kind regards,

Emmy Stigter
(on behalf of all co-authors)

Reply to Anonymous Referee #1

We thank Anonymous Referee #1 for the thorough review. We give our reply (in italic) to the referee comments/ suggestions below.

This paper presents a study focusing on the modelling of snow accumulation and melting in an Himalayan catchment and the response of this catchment under different climate scenarios in terms of snow water equivalent (SWE) and melt runoff. This study addressed an interesting topic in a region where snow storage is crucial for water supply. The authors use data assimilation (Ensemble Kalman Filter, EnKF) of groundbased and remotely-sensed snow data to determine optimal parameters values in their modelling system. These optimal parameters are then used in climate sensitivity tests. My main comments about this study concern (i) the data assimilation method, especially the choice of variables to assimilate and the effects of these choices on final results and (ii) the limits of the climate sensitivity tests carried out with the optimized model. These questions need to be clarified prior to publication in TC. They are listed below (General comments) followed by more specific and technical comments.

General Comments

1) In the study, the EnKF is used to assimilate snow cover area per elevation band and snow depth at two locations. Four parameters are calibrated using the EnKF. My comments on this method concern (i) the choice and benefit of assimilating punctual snow depth measurements and (ii) the assimilation of MODIS snow cover. The assimilation of punctual snow depth is associated with high uncertainties due to the very limited representativeness of punctual snow depth measurement in mountainous terrain (e.g. Grünewald and Lehning, 2015).

We are aware of the high uncertainties related to the limited representativeness of punctual snow depth observations in complex terrain due to local influence of snow drift. We will add the reference, provided by the reviewer, to the revised manuscript for completeness. A key advantage of the EnKF is that it takes into account the uncertainty in the assimilated observations. Several observation uncertainties were tested (variance of 1cm, 16cm and 25cm) on how it influenced the posterior parameter distribution, prior to choosing the final observation uncertainty that is presented in this manuscript (variance of 25 cm). See the next reply for explanation on why we believe that a variance of 25 cm is representative for the uncertainty of punctual snow depth measurements in this case.
In addition we want to emphasize that the assimilation of snow depth observations is only used to calibrate the compaction parameter C_6 and not for calibration of the other three parameters.

For example, wind-induced snow transport can lead to erosion or accumulation of snow at the location of station. What would be the impact of such event when carrying out data assimilation with EnKF? Were the snow depth measurements assimilated in this paper impacted by such event?

Wind-induced snow transport is not included in the snow model presented in this study. If the snow depth measurements are affected by wind-induced snow transport there will definitely be a discrepancy between simulated and measured snow depth that cannot be correctly explained by the model. Using the EnKF for assimilation of measured snow depth to obtain optimal parameter values allows accounting for the uncertainty related to point snow depth measurements. Using a too small measurement uncertainty in the EnKF would result in model parameter values that are too strongly driven by the assimilated snow depth measurements, resulting in implausible values of the model parameters. We checked to which degree the parameter values were driven too strongly by the snow depth measurements as cause of a discrepancy between simulated and measured snow depth. This discrepancy

could (amongst other snow processes) result from wind-induced snow transport. It is difficult to assess whether the station data is influenced by this process based on only measurements of the snow depth. However, results from using different measurement uncertainties showed that a variance of 25 cm (that is used in this study) resulted a mild forcing of the model parameters and plausible values. Therefore, a variance of 25 cm for the measurement uncertainty was assumed to be representative for the uncertainty of punctual snow depth measurements in this case.

The benefit of directly assimilating snow depth measurement is hard to identify throughout the paper. It would be interesting to have results obtained when only snow cover data are assimilated. In the present version of the manuscript, the advantage of simultaneous assimilation of snow cover and depth is not clear enough. Results in Section 3.3.1 and 3.3.2 could be presented (i) without assimilation, (ii) with assimilation of snow cover only and finally (iii) with simultaneous assimilation of snow cover and depth.

The data assimilation is performed in a two-step approach (p8 l14-18). TT, Tlapse and precip were optimized by assimilation of snow extent, whereas C_6 was optimized by assimilation of snow depth. In section 3.3.1 distinction can only be made between the steps 'without assimilation' and 'with assimilation' of snow cover, respectively uncalibrated and calibrated in Figures 3 and 4 because C_6 does not influence the snow extent as it is an parameter that converts SWE in snow depth.
The simulated snow depth without assimilation ('uncalibrated') and after assimilation of both snow depth and snow extent ('calibrated') is already given in Figure 5. The simulated snow depth after assimilation of snow cover only will be included to this figure to show the advantage of assimilation of both snow extent and snow depth (see Figure 1 *below).*

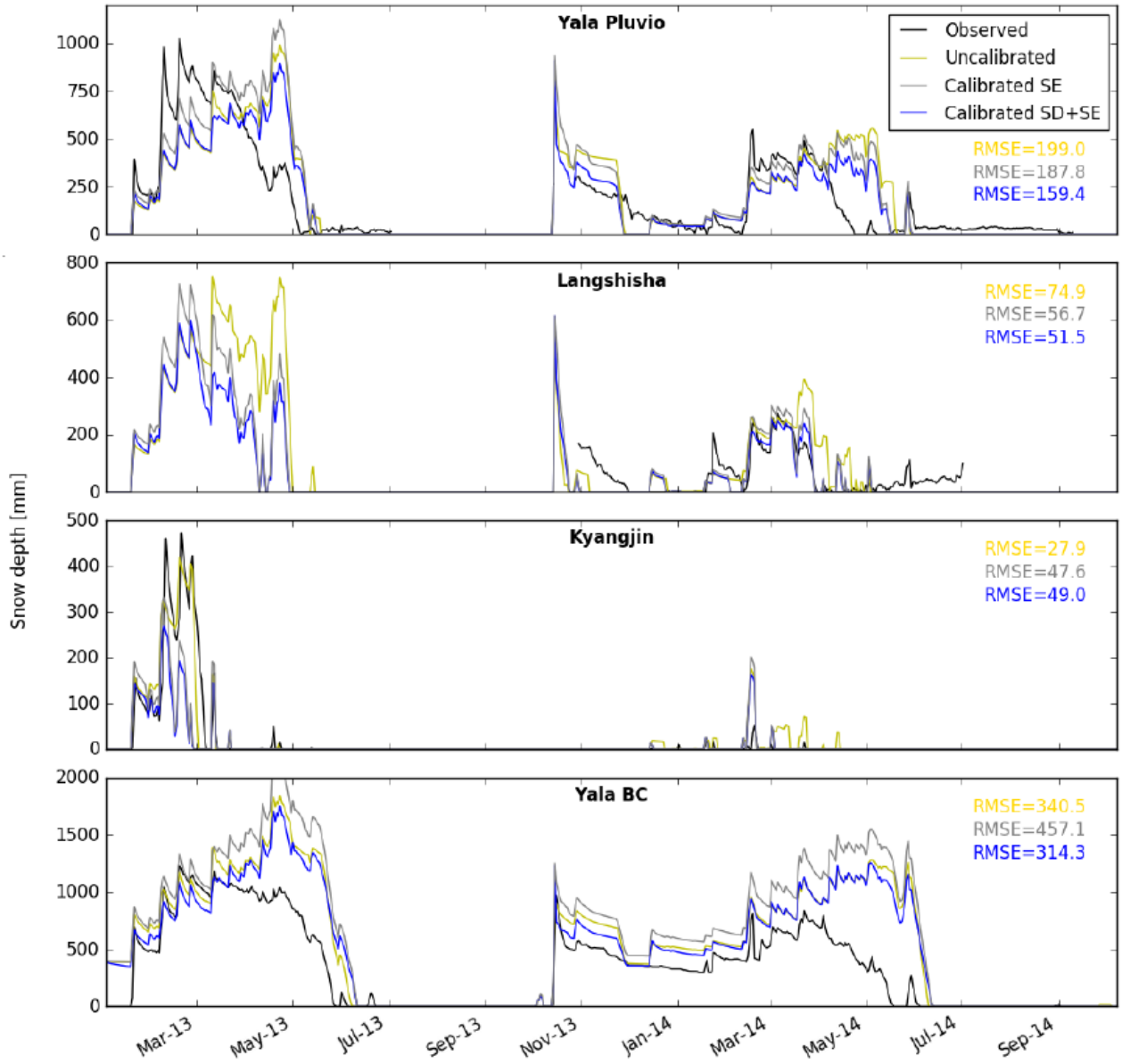

Figure 1 Observed snow depth and modelled snow depth before calibration, after assimilation of snow extent, and after assimilation of both snow depth and snow extent (ensemble mean) at four locations. The RMSE (mm) is given for the fit between modelled (before calibration, after assimilation of snow extent, and after assimilation of both snow depth and snow extent) and observed snow depth.

The assimilation of MODIS snow cover requires an observation operator to convert SeNorge output into simulated snow cover extent. Are the authors using a simple threshold value of SWE or snow depth to determine the presence or the absence of snow? Or are they using depletion curves?

The presence of snow in the model is based on a threshold value of 1 mm swe. This will be added to the manuscript.

MODIS snow cover are averaged per elevation band prior to assimilation. Can the author justify this choice? Indeed, averaging the information per elevation band reduce the information content brought

by MODIS and remove the intra-band variability resulting from (i) the contrast between north-facing and south-facing slopes and (ii) the heterogeneous spatial distribution of precipitation.

The assimilation of snow cover would preferably be performed on a pixel to pixel basis to maintain all information on the spatial distribution of snow cover. However, the EnKF can only be used for continuous values and not for binary values (i.e. snow cover present or not). Therefore it is required to assimilate snow extent (continuous value) into the model. Rather than using the total snow extent for the entire catchment, we chose elevation bands to include more information on the spatial variability of snow cover. Elevation bands were chosen to capture the snow elevation line transition and therefore capture melt dynamics and spatial distribution of precipitation.

2) The authors used the optimized version of their model to carry out climate sensitivity tests. They use the delta method and applied changes in temperature and precipitation for different climate scenarios (Table 3). The authors do not discuss the uncertainties associated with this method. Such discussion is really relevant in a paper dealing with climate sensitivity. The delta method assumes constant changes in space and time for temperature and precipitation. How relevant is this assumption for this region? - Are the changes on temperature and precipitation expected to depend on the season? What are the expected effects for the hydrological cycle in this region? - The authors use the monthly precipitation pattern of Collier and Immerzeel (2015) to spatially distribute precipitation, both in present and future climate. The authors should discuss the validity of this assumption of constant monthly spatial pattern under future climate.

The scope of this study is not to run long-term climate change runs as indeed the study period is too short and might not be representative. This short study period simply does not allow a full-fledged study on climate change scenarios. The focus is rather on the climate sensitivity of the SWE in this study area as a result of changes in temperature and precipitation (using the simple delta method). The study shows the combined effect of changes in air temperature and precipitation. We aim to show patterns that could potentially occur in future under changes in temperature and precipitation. The four RCP4.5 scenarios from Immerzeel et al. (2013) were mainly used to have realistic values for changes in precipitation and temperature.

The spatial distribution of precipitation was kept constant for simplicity. Changes in (spatial distribution of) precipitation are difficult to predict and simulate. In this study we aim to show the importance of knowing the spatial distribution of precipitation in future as we show that increased melt due to increased air temperature can be compensated by an increase in precipitation at high elevation.

So, by no means do we intend to present a climate change impact study, but merely a sensitivity study. In the revised manuscript we will make this clearer. The core of the study is to show how assimilation of snow depth and remotely sensed snow cover in a snow model can lead to a better understanding and quantification of snow water equivalent and snowmelt runoff in an inaccessible, data scarce environment. In particular the title may have given the reviewer the wrong impression about the focus of our study and we will modify the title: 'Assimilation of snow cover and snow depth in a snow model to estimate snow water equivalent and snowmelt runoff in a Himalayan catchment'.

The study period (Jan. 2013 to Sep. 2014) should be compared to the present climatology of the catchment for temperature and precipitation. Is this period considered as cold or warm and wet or dry? Is it representative of the averaged current climate conditions in the Langtang catchment? The author

apply the delta method to a short time period (from a climate perspective) and this short time period must be better characterized.

The study period will be compared to climatology of the catchment. An additional figure (see Figure 2 *below) will be added comparing the study period to the 1988-2009 climatology. However, we want to emphasize again that we do not intend to present a climate change impact study, but merely a sensitivity study.*

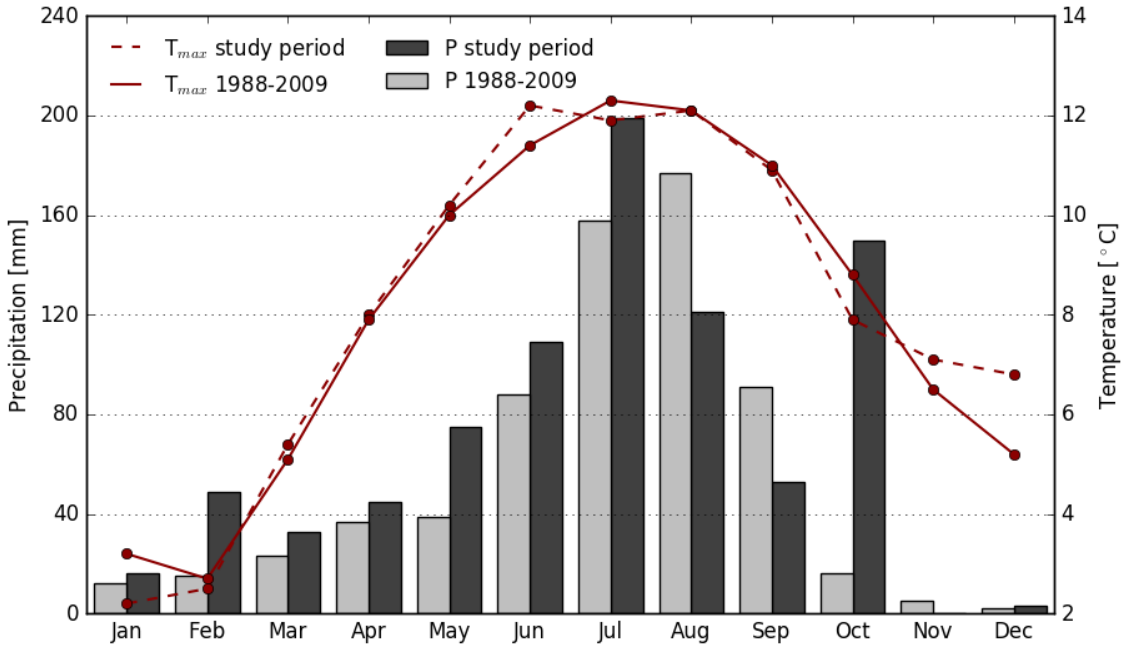

Figure 2 Comparison of maximum temperature (T_{max}) and cumulative monthly precipitation (P) for the study period and the 1988-2009 time series (based on measurements in Kyangjin). The average yearly cumulative precipitation is 853mm and 663mm for the study period and the 1988-2009 time series respectively.

In section 3.5 at P 13 L1, L 13-14 and L 17-18, they authors discuss how the SWE and changes in SWE depend on elevation. This discussion is supported by Figures 7 and 8 that provide maps of SWE for the study period and change of SWE in the different climate sensitivity tests. I recommend the authors to provide complementary figures showing these variables as a function of elevation. It would help the reader to clearly identify the influence of elevation.

An additional figure will be added with boxplots of SWE per elevation zone for the reference run and the four climate sensitivity tests (see Figure 3 *below).*

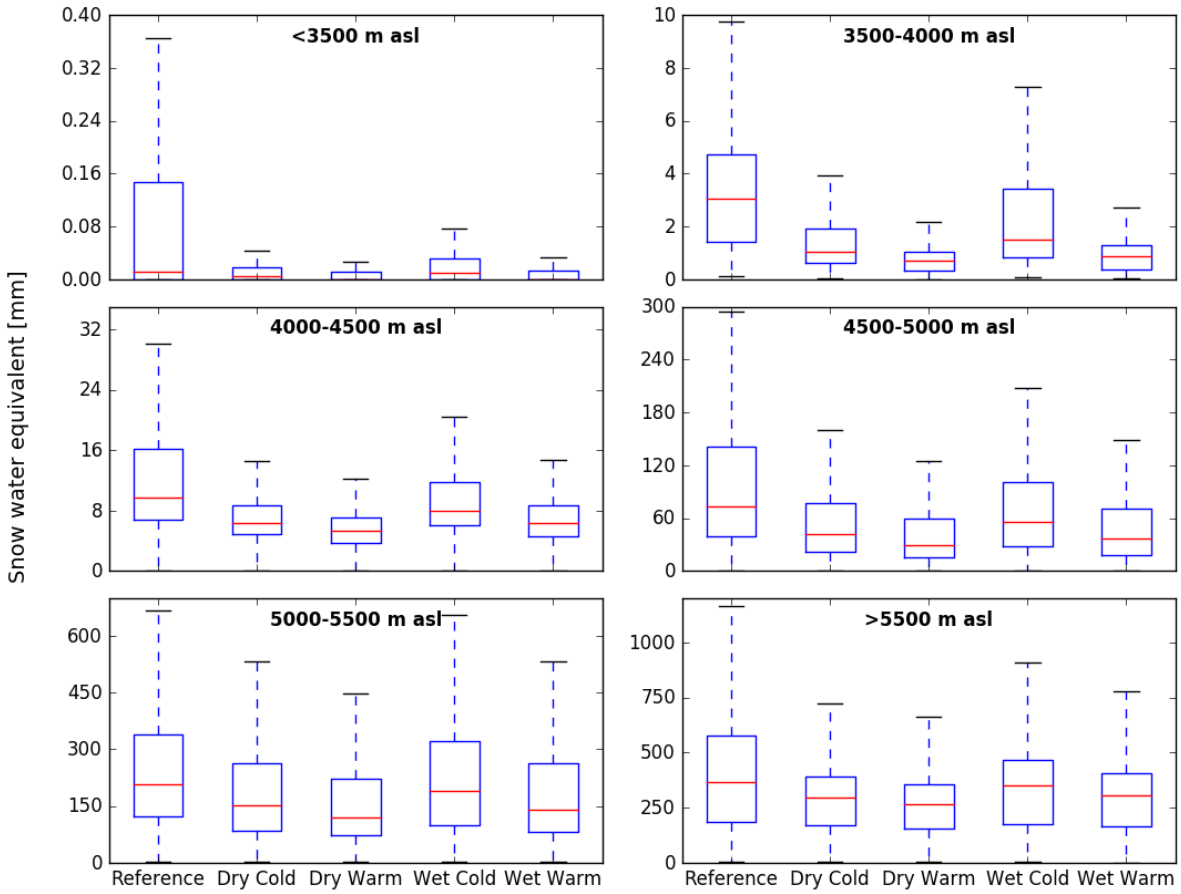

Figure 3 Boxplots of SWE per elevation zone averaged over the simulation period and all ensemble members for the reference run and the four climate sensitivity tests.

Specific comments

Introduction: the introduction is rather short and only presents earlier studies carried out in the Himalayan region. I recommend the authors to write more general paragraphs on (i) data assimilation of ground-based and remotely-sensed snow data in snowpack model and (ii) distributed snowpack modelling applied in mountainous region to simulate the cryospheric and hydrological response of mountain catchments under present and future climate. They should present in this introduction how techniques developed in other mountainous regions could be applied to an Himalayan catchment.

A more extensive introduction will be given, including the points given above.

P 4 L 16-17: the description of the location of the snow depth measurements is confusing. Are the 4 sites measuring snow depth located along the 2 transects? Figure 1 suggests that this is not the case. The authors should clarify this point.

There are 2 transects of surface temperature measurements. Only two out of four snow depth measurements are located along the 2 transects. This will be adjusted.

P 4 L 28: which uncertainties are taken into account with the correction factor precip? Does it include: - uncertainties in solid precipitation measurements at the station due to wind undercatch? - spatial and temporal representativeness across the catchment of the precipitation measured at the station?

Correction factor precip accounts for the uncertainties related to undercatch. This factor does not account for the uncertainties in the representativeness of the chosen monthly spatial distribution of precipitation. We believe that quantifying the uncertainties in spatial distribution is beyond the scope of this study. The fact that we use the monthly spatial precipitation distribution based on a high resolution weather model based Collier and Immerzeel (2015) is already a great improvement over previous studies where fixed lapse rates were used for the entire catchment to regionalize precipitation based on observations of a single station.

P 6 L 3-4: please mention that in Brock et al. (2000) the snow albedo remains constant when the maximum air temperature is below 0 _C.

This will be added.

P 6 L 22: the sentence "Separate transport ... this study" should be reformulated. It suggests than when wet snow avalanches occur the ice and liquid phases are transported separately. This is not the case in the nature. It seems that the authors mentions this point only because seNorge treats separately the solid and the liquid phase in the snowpack.

This was indeed mentioned because seNorge separately treats the solid and liquid phase in the snowpack. The sentence will be reformulated.

P 7 L 8: the runs used for the sensitivity analysis are not clearly described. For each run, are the authors using the model to simulate the evolution of snow cover and SWE over the whole study period (January 2013- September 2014) and the whole catchment? Or are they using different time period and sub-domains?

The sensitivity runs simulate the evolution of snow cover and SWE over the whole study period and the whole catchment. This will be better described.

P 7 L 10: how are computed the mean snow cover extent and snow depth? Are they averaged over the whole period and the whole domain? This point is similar to my previous point regarding the characteristics of the simulations used in the sensitivity analysis.

They are indeed averaged over the whole study area and study period. The description will be improved.

P 7 L 10 (and in the rest of the paper): the author should precise how they compute the snow cover extent from the output of seNorge. Cf my general comments about the observation operator.

See the answer on the general comment.

P 8 L 22-23: how is modified the maximum air temperature in the climate sensitivity tests?

This is a good point. In the previous version of the manuscript we have only perturbed the mean temperature forcing, but for the revised manuscript we have now imposed the same delta change on the maximum temperatures. The impact is however minimal and only for the dry warm case, a difference of a few percent in SWE is simulated compared to the previous version. This is because the maximum temperature is only used in the albedo decay algorithm, so when Tmax is higher, then the albedo decay will start a bit earlier, however the impact is minimal in these sensitivity tests. Figures 8 and 9 will be updated in the revised manuscript with the climate sensitivity tests including perturbation of Tmax.

P 10 L 19-25: this paragraph should also discuss model results in the elevations zones above 5000 m. For example, could the author discuss the differences between summer 2013 and 2014 in terms of snow extent in the elevation zones 5000-5000 m and >5500 m? What can explain the underestimation of SCE in these zones for summer 2013 whereas better results are achieved in summer 2014?

We will add a paragraph to the results and discussion section, where we discuss the potential reasons for those high altitude differences.

P 10 L 29: differences in classification accuracy with and without calibration are hard to identify on Figure 4. A map of differences of classification accuracy could help the reader to better identity the regions where large differences are found between the two simulations.

Before calibration the snow model already shows high performance in simulating snow cover (Figure 4a). After calibration there is only a modest improvement in accuracy in most regions, whereas there is a slight decrease in performance in few other regions. The small changes in performance are therefore indeed hard to identify. The only pronounced improvement is in the lower area on the northern slope and this improvement also shows from Figure 3. A difference map was tested, but resulted in rather chaotic patterns of small increases and decreases in accuracy in steep terrain and therefore does not help visualization and interpretation. Given the little information content, the fact that elevation dependent improvements are already shown in Figure 3 and since we already add a new figure (boxplots) we have decided not to include the proposed figure in the revised manuscript.

P 10 L 30-31: the authors associate the low classification accuracies in the northern part of the catchment with model errors due the avalanching parametrization. However, it seems that this difference can also arise from errors in the meteorological forcing used to drive seNorge. For example: (i) errors in precipitation phase and amount, (ii) errors in the spatial distribution of precipitation. Indeed, the spatial distribution of precipitation is based on monthly precipitation patterns derived from Collier and Immerzeel (2015). For a given precipitation event, the spatial distribution of precipitation can vary from the monthly pattern from Collier and Immerzeel (2015) and strongly affect the snow cover. Please add a discussion about the different potential sources of error.

This is correct and a more complete description of reasons for low classification errors will be added to the discussion.

P 11 L 23-24: please consider reformulating the last sentence of this paragraph. Indeed,
the improvement for Kyangjin in 2014 is not really clear.

This will be reformulated.

P 11 L 25: the authors point out the lack of independent stations for the evaluation of snow depth and SWE. Are glacier mass balance data available for a glacier in this catchment to bring complementary values for evaluation? For example, winter mass balance data can provide interesting evaluation on the cumulated precipitation during the winter.

The yearly mass balance is available for Yala glacier, which is a clean-ice glacier positioned in the study area. However, the yearly mass balance is negative. As only snowmelt is simulated, and no glacier melt, it is impossible to simulate a negative mass balance with the snow model. Therefore no comparison was made between output of the snow model and available mass balance data.

Though, an extra data set of snow depth measurements will be used (Yala BC; see Figure 1 *above) to improve the validation of the simulated snow depth. This will be added to the revised manuscript.*

P 11 L32: the absence of underestimation or overestimation concerns snow depth and not SWE.

This will be adapted.

P 12 L 5-30, Section 3.4: This section does not contain new and original results and only presents the effect of well-established parametrizations introduced in seNorge to improve the snowpack dynamics without comparison with measurements. I recommend the authors to remove the discussion concerning the snow compaction and the snow albedo since it does not bring additional value to their paper.

This section will be removed from the manuscript.

Concerning the avalanche parametrization, the discussion at lines 7-10 (P 12) suggests that avalanching strongly affects the simulation results. It would be really interesting if the authors could illustrate how the avalanching parametrization improves the representation of the snow depth distribution in the model. Figure 7 shows that, in the simulations, snow accumulates at the bottom of the steep slopes of the catchment. Are these zones of additional snow accumulation identified on the LandSat images at 30-m resolution? Such discussion on avalanche processes and a comparison with remotely-sensed observation would substantially improve the quality of this section on snow processes. Otherwise, I recommend to remove this section from the paper.

The snow accumulation zones are not clearly visible in Landsat 8 imagery. This is caused by i) the shadow in the steep areas, ii) a too small extent of the accumulation zones, and iii) potentially a wrong timing of the acquisition date. Therefore a comparison of simulated and remotely sensed snow cover in the deposition zones is impossible. Based on extensive field experience we know that avalanches regularly occur at these steep walls and that snow is deposited downslope these steep walls. The walls are too steep to have a substantial snow depth. Including avalanching in the model improves the snow redistribution as there can be no unrealistic accumulation of snow in these steep zones. Although, there is no possibility to support this with Landsat 8 imagery, we respectfully disagree with the recommendation of removing this section, as we believe it is important and improves the distribution of snow in the model.

Technical comments
Text

P 16 L 25: modify the reference to Immerzeel et al. (2014)

This will be modified.

References (not included in the submitted manuscript)

Grünewald, T., Lehning, M. (2015). Are flat-field snow depth measurements representative? A comparison of selected index sites with areal snow depth measurements

This will be included.

Reply to Hendrik Wulf Referee #2

We thank Hendrik Wulf for his extensive comments and positive feedback. All the suggested typographical revisions will be adjusted for the revised manuscript. Below we summarize the comments given by the reviewer and our replies (italic)

Dear Editor, author and co-authors.
This paper presents an illuminating analysis in the spatial (and temporal) distribution of SWE in the Langtang Valley, Nepal, and the findings are useful to anyone investigating the hydroclimatic phenomena and variability from the Hindu Kush to the Eastern Himalaya. Unique to this study is the use of actual field observation (a rarity in the Himalayas) and their incorporation in a modeling approach for SWE. The explication could be improved, and I have marked up the manuscript. But although my comments are extensive, they are straightforward, so I do not feel I need to see the paper again.
I look forward to reading the published version.
Kind regards, Hendrik Wulf

p1 l20 Why only in the Himalayas? Isn't this of general interest in complex snowy terrain?

It is a new approach for the Himalayas and therefore of main interest for the Himalayas. However, it is indeed of general interest for complex terrain. We will stress this in the revised manuscript.

p1 l22 Why do you assume an increase in precipitation at high elevation in the future? Is that true for all your four scenarios or which one do you focus on here? I find this a little bit confusion. A suggestion. Pick the most likely out of your four scenarios and provide the impact of the change with some numbers. So, what is the change in temperature and what would be the impact on SWE.

Immerzeel et al. (2013) analysed all available CMIP5 simulations for the emission scenario RCP4.5 for the Langtang catchment. They selected the four extremes from the RCP4.5 ensemble members ranging from dry to wet and from cold to warm. We used their projected changes in precipitation and temperature (Table 3). Their projected changes show both a decrease and increase in precipitation. We want to emphasize that we do not intend to perform a climate change impact study but merely a sensitivity study (see also the reply to reviewer #3). We describe the patterns that result from the climate sensitivity tests (including increase and decrease in precipitation). There is not per definition a climate sensitivity test that is most likely. Therefore a description is given of the most interesting results from the sensitivity tests, i.e. patterns that occur as result of changes in temperature and precipitation.

p1 l25 Some kind of closing sentence is missing with regard to the opening. For example, snow as important water storage in the Langtang Valley is projected to decrease by X% assuming a temperature increase of X°C, which has implications on ...

No numbers are presented here to prevent the thought that we actually performed a climate impact study. We rather performed climate sensitivity tests and we intend to mainly describe qualitative results.

p2 l11 "No information" is not quite correct. Using the "inverse melt" approach by Molotch et al. (2009) you can gain information on SWE. I used this simple approach in the western Himalaa and it worked quite well (Wulf et al. 2016)

MolotchNP,NorteD.ReconstructingsnowwaterequivalentintheRioGrandeheadwatersusingremotelysensedsnowcoverdataandaspatiallydis-tributedsnowmeltmodel.HydrolProcess2009;1089:1076–89.http://dx.doi.org/10.1002/hyp.7206.

It will be changed into 'limited information'. The given references will be added. We appreciate the suggestion.

p2 l12 Do you refer to currently recorded data or available data? I am aware of continuos data records in the Indian Himalaya, which are not publicly available. Further efforts existed in the central Himalaya. There are publications on snowfall and SWE in the Himalaya. See Putkonen et al.(2004) and Wulf et al. (2016).

Putkonen, J.K.
Continuous snow and rain data at 500 to 4400 m altitude near Annapurna, Nepal, 1999-2001
(2004) Arctic, Antarctic, and Alpine Research, 36 (2), pp. 244-248. Cited 38 times.
https://www.scopus.com/inward/record.uri?eid=2-s2.0-9944234078&partnerID=40&md5=c770cdf50445a4762d9b9757e46f56de

Wulf, H., Bookhagen, B., Scherler, D.
Differentiating between rain, snow, and glacier contributions to river discharge in the western Himalaya using remote-sensing data and distributed hydrological modeling
(2016) Advances in Water Resources, 88, pp. 152-169. Cited 1 time.
https://www.scopus.com/inward/record.uri?eid=2-s2.0-84954410375&doi=10.1016%2fj.advwatres.2015.12.004&partnerID=40&md5=a48d65ad590068da9a363c979cd7b15b

This sentence will be rephrased: 'Currently there is limited information of SWE for the Himalayas'.
We were referring to available data sets. Thank you for making us aware of this interesting literature. The references will be added to the revised manuscript.

p2 l30 You highlight the differences between low-elevation and high-elevation precipitation at the southern slopes. Is there also a north south gradient in precipitation?
See the work of Ana Barros.

We will rephrase this as follows:
There is a strong interaction between the orography and precipitation patterns. During the monsoon, at the synoptic scale, there is a decreasing trend from south to north during the monsoon, but at smaller scales there are more local orographic effects associated to the aspect of the main valley ridges (Barros et al, 2004) that determine the precipitation distribution. During the monsoon precipitation mainly accumulates at the south western slopes near the catchment outlet at low elevation. Winter westerly events can also provide significant snowfall. Snow cover has strong seasonality with extensive, but sometimes erratic, winter snow cover and retreat of the snowline to higher elevations during spring and summer and less snow cover. During the winter precipitation mainly accumulates along high-elevation southern-eastern slopes (Collier and Immerzeel, 2015).

p3 l25 I would recommend to use the more general formulation: NDSI (Green-SWIR1) / (Green+SWIR1). This way you could reuse the equation for L8, too.

The formula for the NDSI will be changed into a more general formula using green and SWIR.

p4 l2 How many cloud free scenes out of how many total scenes did you use in the end? How well did they cover the snow melt period?

10 out of 34 available Landsat 8 images were used for validation of the snow model. The coverage can be seen in Figure 3.

p4 l14 What did you use the surface temperature for?

We used the surface temperature measurements for distinguishing between snow covered and no-snow covered periods at a point-scale. These point measurements are used to validate the remotely sensed snow cover. This is described in the results and discussion section.

p4 l16 Surface or air temperature?

Surface temperature. This will be revised.

p4 l25 What are the lapse rate values? How good do they describe the variation between the temperature stations? Do these values vary during the year?

The temperature lapse rates agree with values presented in the study of Immerzeel et al. (2014). There is seasonal variation in the lapse rates similar to Immerzeel et al. (2014).

p4 l29 How uncertain are these temperature measurements?

We do not refer to the uncertainty in the temperature measurements, but to the uncertainty of the derived temperature lapse rate. We will clarify this in the revised manuscript.

p5 l9 How did you incorporate the 500m MODIS pixel in your model? Simple upscaling?

The 500m MODIS pixels were resampled to 100m to fit the spatial resolution of the model.

p6 l10 Do you have any idea by which degree your snow depth measurements are affected by snow redistribution?

The snow depth measurements are not influenced by avalanching, though there might be some influence from wind transport. However, when assimilating the snow depth measurements, an uncertainty was added to the snow depth measurement to account for the uncertainty that results from wind-induced snow deposition and erosion. See also the reply to reviewer 1.

p7 l29 I assumed you use a distributed modelling approach. Do I rightly assume that snowmelt is generated per elevation band not per model pixel? Please clarify.

Snowmelt is generated per pixel. This will be clarified.

p7 l30 Landsat snow cover data is not used in your model only the validation?

Yes, it is used as an independent validation of the simulated snow cover.

p7 l31 Why did you not choose equal area breakpoints to ease the direct comparison?

We want to characterize the snow cover per elevation zone. Equal area breakpoints resulted in unevenly distributed elevation zones given the catchment's hypsometry. Therefore, unequal area breakpoints were chosen to have approximate equal elevation intervals.

p8 l24 What does this mean?

Immerzeel et al. (2013) analysed all available CMIP5 simulations for the emission scenario RCP4.5 and extracted precipitation and temperature trends. They selected 4 models that ranged from dry to wet and from cold to warm for the Langtang catchment. The changes in in temperature (°C) and precipitation (%) are extracted from the 4 models. The projected annual change is for 2021-2050 relative to 1961-1990. This will be clarified in the manuscript.

p8 l25 What about the dry to dryer scenario is the summer monsoon and/or westerlies weaken?

It is assumed that both occur. However, precipitation is much more substantial during monsoon and therefore the dry to dryer climate sensitivity tests mainly influence the monsoon precipitation.

p8 l26 I recommend to clearly distinguish between your results and the discussion. This is common scientific practice.

We believe that combining these sections improves the readability in our case. It is nowadays also not uncommon to combine the results and discussion, so we propose to keep it as it is..

p9 l12 The other studies compared MOD10A1 data. The simplification of MOD10A2 surely introduces additional errors. Larger uncertainties also stem from large viewing angles, which can increase the observation area by a factor of 10 for MODIS. See Dozier et al. 2008.

Both notes will be added to the manuscript.

p9 l17 I would assume that the snow observation on the ground differs, too. I honestly doubt that relief introduces such a big error if the satellite data is geocoded correctly. USGS does a good job here for their TOA products.

In situ snow observations indeed result in additional uncertainty. This is already described in the manuscript (p9 l17-22). The relief is causing high spatial variability in snow cover. It is believed that the spatial resolution of MOD10A2 snow cover does not capture this spatial variability. We do not refer to correct geocoding. This will be clarified.

p10 l6 Any values (before and after calibration) would be much appreciated.

These values can be found in Table 6. We already refer to this table in the manuscript (p10 l2).

p15 l4 Do you mean: "increased melt due to higher temperatures"?

Yes, this will be revised.

p18 l14 Nice figure. However, the map is missing coordinated and an inset to locate it in the Himalayas.

The figure will be revised so it addresses these comments (See Figure 1 *below).*

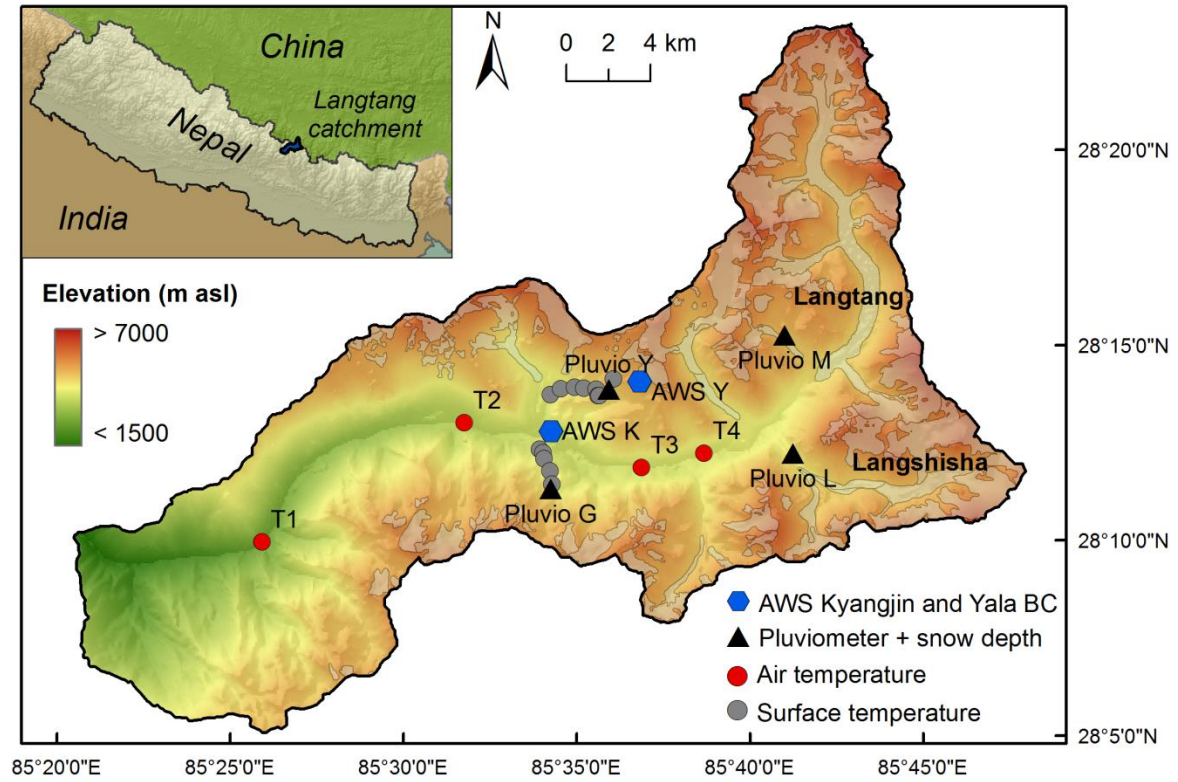

Figure 1 Study area with the locations of the in situ observations. Langtang and Langshisha refer to two main glaciers in upper Langtang Valley.

p19 l1 Which are these locations and what is their respective elevation? Why is the surface temperature above zero for some snow cover periods? How certain are you about the snow free periods during sprng the upper example (Yala 5)? Are late snowfall events more common in spring as compared to the winter period?

The locations and elevation are given in Table 1. The table number will be added to the figure description.
The above zero temperature results from the uncertainty of the surface temperature measurements. The short snow free periods during spring for Yala 5 are associated with the uncertainty of the temperature measurements. During winter precipitation events are rare, whereas during spring late snowfall events are common.

In Figure 3 there seems to be quite a mismatch between Landsat and MODIS. How do you explain this difference?

The coarse resolution of MODIS does not allow observing the high spatial variability in snow cover. MODIS snow cover shows full snow cover, whereas Landsat shows higher spatial variability (also some no-snow cover) at higher elevations. This results in a mismatch between MODIS and Landsat.
In addition the Landsat 8 derived snow maps are influenced by shading. Shaded snow covered area is erroneously mapped as no-snow areas and therefore also results in underestimation of snow cover by landsat compared to MODIS.

p21 l5 Could you indicate these locations in your Fig. 1? I would opt for dashed and solid lines to improve the distinction in b/w printouts.

These locations are already indicated in Table 1 and Figure 1.
The figure will be updated and will contain more lines (see reply to reviewer 1). Therefore we believe that dashed and solid lines will not enhance distinguishing between different lines.

Do the values in Figure 7 match the glacier snow accumulation rate at high elevations? What is the maximum SWE value you got?

We do not know the snow accumulation rate at high elevations as there is only yearly mass balance data available that also includes ablation.
The maximum SWE will be given in an additional figure showing box plots of SWE values per elevation zone (see reply to reviewer 1).

In Figure 8 you have (white) space enough to write the different scenarios directly into the figure (as a subfigure headline. Please also state here what wet, dry, cold and warm refer to.

This will be adjusted. Reference will be made to Table 3 to clarify the different climate sensitivity tests mentioned in this figure.

p24 l1 How was runoff measured? Which method? Does melt also include glacier melt? If not, it is better to refer to snow melt.

Runoff was not reliably measured in the field and is therefore not included in this study. In the model it is assumed that all runoff, for each pixel, collects at the catchment outlet for each time step without applying routing.
Melt includes only snowmelt, although it includes snowmelt on glaciers. The legend will be adapted to snowmelt.

References:
Barros, A. P., Kim, G., Williams, E. and Nesbitt, S. W.: Probing orographic controls in the Himalayas during the monsoon using satellite imagery, Nat. Hazards Earth Syst. Sci., 4(1), 29–51, doi:10.5194/nhess-4-29-2004, 2004.

Reply to Anonymous Referee #3

We thank Anonymous Referee #3 for the thorough review. We provide our reply to the referee suggestion/comments below (in italics)

General: The paper presents an interesting analysis of current and future snow dynamics for the Langtang catchment in the Himalayas (Nepal). The paper is well-written and follows a clear line of argumentation. The approach of including as much as possible local and satellite data has a lot of merit. At the same time, I have major concerns about the methodology as detailed in the following.

We appreciate this positive feedback and below we explain our choice for the methodology and we will cover the concerns outlined by Anonymous Referee #3.

In my opinion, climate change scenario calculations based on simple (parameterized) snow models are unreliable as they necessarily present an extrapolation beyond the state for which the models have been calibrated. The problem with such simple snow models has been exemplarily shown by Magnusson et al. (2011). In this publication, a physics-based model and a model similar to seNorge are shown to produce similar results for a current climate but very diverging results for climate change scenarios.

We agree that in a perfect world a full energy balance model driven by observational data would be the ideal basis for a climate change impact study. However, the core of our paper is to show how a smart integration of remotely sensed snow cover imagery, data assimilation and a snow model can result in improved spatial estimate of snow water equivalent. We show the benefit of assimilating snow cover and snow depth into a snow model that simulates SWE and snowmelt runoff. This data assimilation approach would not have been computationally feasible in a physically-based model, due to the extensive parameterization and high number of dependent state variables. Previous approaches for snow(melt) modelling in the Himalaya dominantly relied on modelling a melt flux from a snow covered area (lacking information of SWE; e.g. Bookhagen and Burbank, 2010; Immerzeel et al., 2009) or used an inversed melt approach (Wulf et al., 2016) *which only provides information on the maximum SWE for a snow season. This study is novel as both the snow water equivalent and snowmelt runoff of a Himalayan snowpack is explicitly simulated. This novel approach then also allows assessing changes in SWE and snowmelt runoff as result of changes in temperature and precipitation. This study is not intended to be a full-fledged study on climate change impacts as the data set is short and detailed information on changes in temperature and precipitation (patterns) is lacking (as already pointed out by RC1). In addition we are aware of the limitations regarding the use of parameterized snow models for climate change scenarios. Therefore we present climate sensitivity tests, showing the sensitivity of SWE and snowmelt runoff to changes in temperature and precipitation. This gives additional information about the sensitivity of the Himalayan snowpack under a changing climate, without stressing the use of a parameterized snow model for purposes that it is unsuitable for.*

We agree that in particular the title may have given the reviewer the wrong impression about the focus of our study and we will modify the title to: 'Assimilation of snow cover and snow depth in a snow model to estimate snow water equivalent and snowmelt runoff in a Himalayan catchment'. In addition we will make it clearer in the manuscript that it is not a climate change impact study but merely a sensitivity experiment. We will also include a paragraph in the introduction on physics based versus "simple" snow models and we will include the Magnusson et al. (2011) reference.

The data assimilation via Kalman filtering potentially makes the modelling in the presented paper even more vulnerable to extrapolation than when using robust standard parameters. This is a major objection I have towards the methodology.

We agree that the Ensemble Kalman Filter (EnKF) has the potential to increase the vulnerability of a snow model to extrapolation as the model could be parameterized to fit the current climate and not future climate. However, in addition to our previous reply, we believe that this will be limited in this particular case because the posterior parameter distribution shows plausible values for the parameters. Using the EnKF actually provides valuable insight in the parameter and simulation uncertainty, compared to a deterministic simulation. In our case the narrow posterior distribution of parameter values together with plausible values shows the robustness of the parameterized snow model.

What is aggravating the problem described above is that the paper appears to completely ignore a large body of literature, which is based on physics-based snow modelling of climate change impacts. This has already been pointed out by RC1. I do not want to necessarily suggest that a paper based on temperature index modelling of future climate needs to be rejected in all cases. But if such an analysis is retained it needs to show a very careful assessment of potential errors through extrapolation and a discussion and comparison with results obtained with physics-based models.

We refer to our reply about the focus of our paper and we do not see where reviewer 1 indicated that physical-based snow models are a prerequisite for climate change impact studies, however we agree that a more thorough review regarding the pros and cons of physical-based models and temperature index models would improve the manuscript and provides a better context for our choices. In the revised manuscript a more extensive review will be given in the introduction about different model approaches (physical-based vs temperature index) and the results from previous studies. In the discussion the potential errors arising from non-stationarity and the extrapolation by a parameterized model will be addressed and placed in a proper context.

Computational restrictions do no longer prevent physics-based models to be applied to larger areas and for significant climate change studies. A recent example is Marty et al. (2017), which has just appeared in TC and which is a good starting point for the authors to find additional studies, which they need to discuss in context of their analysis.

Indeed there are no longer computational restrictions that prevent the use of physics-based models for larger areas. However, it is the limited data availability in the Himalayas that constrains the use of physics-based models. Physics-based models require extensive input data that is often unavailable in the Himalayas. Therefore it is necessary to use a parameterized snow model (requiring less input data) to perform SWE and snowmelt analysis of a Himalayan snowpack. To the authors' knowledge there is currently no study available that simulates the snowpack spatially distributed with a physics-based model for a Himalayan catchment. This supports our choice for a simpler approach.
We thank the referee for providing this interesting study. It will definitely help us to find more literature and it will enable us to put our results in a better context.

Interestingly, the results of the latter study (for the Alps) qualitatively agree with what the authors find for Langtang and this is a good sign. But this also means that the results are qualitatively not new and quantitatively highly uncertain for the argument presented above.

The same qualitative results show the capability and potential of the parameterized snow model to simulate climate sensitivity of SWE and snowmelt runoff. We disagree that these results are not new. To our opinion assimilating snow depth and remotely sensed snow cover into a snow model with parametrizations on melt modelling, albedo decay, avalanching, and snow compaction, and its first time application in a remote Himalayan catchment with the aim to understand the spatial patterns and climate sensitivity of SWE is quite novel.

This is my major point about the paper and I otherwise agree with the points raised by RC1.

See the replies to the points raised by RC1.

In general, presentation, figures and form of the paper are already at a very advanced state and almost without problems.

References:

Magnusson, J., Farinotti, D., Jonas, T. and Bavay, M. (2011), Quantitative evaluation of different hydrological modelling approaches in a partly glacierized Swiss watershed. Hydrol. Process., 25: 2071–2084. doi:10.1002/hyp.7958

Marty, C., Schlögl, S., Bavay, M., and Lehning, M.: How much can we save? Impact of different emission scenarios on future snow cover in the Alps, The Cryosphere, 11, 517-529, doi:10.5194/tc-11-517-2017, 2017.

References:

Bookhagen, B. and Burbank, D. W.: Toward a complete Himalayan hydrological budget: Spatiotemporal distribution of snowmelt and rainfall and their impact on river discharge, J. Geophys. Res. Earth Surf., 115(3), 1–25, doi:10.1029/2009JF001426, 2010.

Immerzeel, W. W., Droogers, P., de Jong, S. M. and Bierkens, M. F. P.: Large-scale monitoring of snow cover and runoff simulation in Himalayan river basins using remote sensing, Remote Sens. Environ., 113(1), 40–49, doi:10.1016/j.rse.2008.08.010, 2009.

Wulf, H., Bookhagen, B. and Scherler, D.: Differentiating between rain, snow, and glacier contributions to river discharge in the western Himalaya using remote-sensing data and distributed hydrological modeling, Adv. Water Resour., 88, 152–169, doi:10.1016/j.advwatres.2015.12.004, 2016.

~~Climate sensitivity of~~Assimilation of snow cover and snow depth into a snow model to estimate snow water equivalent and snowmelt runoff in a Himalayan catchment

Emmy E. Stigter[1], Niko Wanders[2], Tuomo M. Saloranta[3], Joseph M. Shea[4,5], Marc F.P. Bierkens[1,6], Walter W. Immerzeel[1]

[1] Department of Physical Geography, Utrecht University, The Netherlands
[2] Department of Civil and Environmental Engineering, Princeton University, United States
[3] Norwegian water resources and energy directorate (NVE), Oslo, Norway
[4] International Centre for Integrated Mountain Development, Kathmandu, Nepal
[5] Centre for Hydrology, University of Saskatchewan, Canada
[6] Deltares, Utrecht, The Netherlands

Correspondence to: Emmy E. Stigter (e.e.stigter@uu.nl)

Abstract. Snow is an important component of water storage in the Himalayas. Previous snowmelt studies in the Himalayas have predominantly relied on remotely sensed snow cover. However ~~this~~, snow cover data provides no direct information on the actual amount of water stored in a snowpack i.e. the snow water equivalent (SWE). Therefore, in this study remotely sensed snow cover was combined with in situ ~~meteorological~~ observations and a modified version of the seNorge snow model to estimate (climate sensitivity of) SWE and snowmelt runoff in the Langtang catchment in Nepal. Snow cover data from Landsat 8 and the MOD10A2 snow cover ~~maps~~product were validated with in situ snow cover observations provided by surface temperature and snow depth measurements resulting in classification accuracies of 85.7% and 83.1% respectively. Optimal model parameter values were obtained through data assimilation of MOD10A2 snow maps and snow depth measurements using an Ensemble Kalman filter. The approach of modelling snow depth in a Kalman filter framework allows for data-constrained estimation of ~~SWE~~snow depth rather than snow cover alone and this has great potential for future studies in complex terrain, especially in the Himalayas. Climate sensitivity tests with the optimized snow model show a strong decrease in SWE in the valley with increasing temperature. However, at high elevation a decrease in SWE is (partly) compensated by an increase in precipitation, which emphasizes the need for accurate predictions on the changes in the spatial distribution of precipitation along with changes in temperature. Finally the climate sensitivity study revealed that snowmelt runoff increases in winter and early melt season (December to May) and decreases during the late melt season (June to September) as a result of the earlier onset of snowmelt due to increasing temperature.

1 Introduction

In the Himalayas a part of the precipitation is stored as snow and ice at high elevations. This water storage is affected by climate change resulting in changes in river discharge in downstream areas (Barnett et al., 2005; Bookhagen and Burbank,

2010; Immerzeel et al., 2009, 2010). The Himalayas and adjacent Tibetan Plateau are important water towers, and water generated here supports the water demands of more than 1.4 billion people through large rivers such as the Indus, Ganges, Brahmaputra, Yangtze and Yellow (Immerzeel et al., 2010). So far, the main focus has been on the effect of climate change on the glaciers and the resulting runoff. However, snow is an important short-term water reservoir in the Himalayas, which is released seasonally contributing to river discharge (Bookhagen and Burbank, 2010; Immerzeel et al., 2009). The contribution of snowmelt to total runoff is highest in the western part of the Himalayas and lower in the eastern and central Himalayas (Bookhagen and Burbank, 2010; Lutz et al., 2014).

Although Himalayan snow storage is important for the water supply in large parts of Asia, in situ observations of snow depth are sparse throughout the region. Many studies benefit from the continuous snow cover data retrieved from satellite imagery to estimate snow cover dynamics or contribution of snowmelt to river discharge ~~(Bookhagen and Burbank, 2010; Gurung et al., 2011; Immerzeel et al., 2009; Maskey et al., 2011).~~(Bookhagen and Burbank, 2010; Gurung et al., 2011; Immerzeel et al., 2009; Maskey et al., 2011; Wulf et al., 2016). Studies about snowmelt in the Himalayas have predominantly relied on remotely sensed snow cover and a modelled melt flux estimating melt runoff resulting from this snow cover (e.g. ~~Bookhagen and Burbank, 2010; Immerzeel et al., 2009; Tahir et al., 2011). However, this provides no~~Bookhagen and Burbank, 2010; Immerzeel et al., 2009; Tahir et al., 2011; Wulf et al., 2016). However, this approach provides no or limited information on snow water equivalent (SWE), which is an important hydrologic measure as it indicates the actual amount of water stored in a snowpack. ~~Currently there is no reliable information~~SWE can be reconstructed based on integrating a simulated melt flux over the time period of remotely sensed observed snow cover. However, this method provides only information on the peak SWE value and introduces errors when snowfall occurs during the melt season (Durand et al., 2008; Molotch, 2009; Molotch and Margulis, 2008). Currently there is only limited reliable information available on SWE for the Himalayas ~~(Lutz et al., 2015).~~(Lutz et al., 2015; Putkonen, 2004). SWE can be retrieved with passive microwave remote sensing, but the results are highly uncertain, especially for mountainous terrain and wet snow (Dong et al., 2005). In addition the spatial resolution is coarse and therefore inappropriate for catchment scale studies in the Himalayas. Estimating both the spatial and temporal distribution of SWE and snowmelt is important for flood forecasting, hydropower and irrigation in downstream areas.

Selection of a suitable snow model is critical to correctly represent snow cover and SWE. Snow models of different complexity exist and can be roughly divided into physical-based and temperature-index models. Several studies have compared snow models of different complexity and their performance. Physical-based models typically outperform temperature-index models for snowpack runoff simulation on a sub-daily timescale (Avanzi et al., 2016; Magnusson et al., 2011; Warscher et al., 2013). However, physical-based and temperature-index models have similar ability to simulate daily snowpack runoff (Avanzi et al., 2016; Magnusson et al., 2015). Avanzi et al. (2016) showed that the use of a temperature-index model does not result in a significant loss of performance in simulation of SWE and snow depth with respect to a physical-based model. Even though physical-based models outperform temperature-index models in some cases,

temperature-index models are often preferred as data requirements and computational demand are lower. Especially in the Himalaya, data availability constrains the choice of a snow model.

Assimilation of remotely sensed snow cover and ground-based snow measurements have been proved to be an effective method to improve hydrological and snow model simulations (Andreadis and Lettenmaier, 2006; Clark et al., 2006; Leisenring and Moradkhani, 2011; Liu et al., 2013; Nagler et al., 2008; Saloranta, 2016). Although different data assimilation techniques exist, Kalman Filters techniques are often selected, due to their relatively low computation demand. They estimate the most likely solution using an optimal combination of observations and model simulations. Especially in catchments with strong seasonal snow cover, assimilation of remotely sensed snow cover is expected to be most useful as a result of fast changing conditions in the melting season (Clark et al., 2006).

The aim of this study is to estimate SWE and snowmelt runoff in a Himalayan catchment by assimilating remotely sensed snow cover and in situ snow depth observations into a modified version of the seNorge snow model (Saloranta, 2012, 2014, 2016). Climate sensitivity tests are subsequently performed to investigate the change of SWE and snowmelt runoff as result of changing air temperature and precipitation. The approach of modelling snow depth allows to validate the quantity of simulated snow rather than snow cover alone and is a new approach in Himalayan snow research.

2 Methods and data

2.1 Study area

The study area is the Langtang catchment, which is located in the central Himalaya approximately 100 km north of Kathmandu (Figure 1). The catchment has a surface area of approximately 580 km^2 from the outlet near Syabru Besi upwards. The elevation ranges from 1406 m above sea level (asl) at the catchment outlet to 7234 m asl for Langtang Lirung, which is the highest peak in the catchment. The climate is monsoon-dominated and 68% to 89% of the annual precipitation falls during the monsoon (Immerzeel et al., 2014). ~~The spatial patterns in precipitation are seasonally contrasting. During the monsoon precipitation mainly accumulates at the southern slopes and near the catchment outlet at low elevation. However, during the winter precipitation mainly accumulates along high elevation southern~~Spatial patterns in precipitation are seasonally contrasting, and there is a strong interaction between the orography and precipitation patterns. At the synoptic scale, monsoon precipitation decreases from south to north, but at smaller scales local orographic effects associated to the aspect of the main valley ridges (Barros et al., 2004) determine the precipitation distribution. Numerical weather models suggest that monsoon precipitation mainly accumulates at the southwestern slopes near the catchment outlet at low elevation, while winter precipitation mainly accumulates along high-elevation southern-eastern slopes (Collier and Immerzeel, 2015). Winter westerly events can also provide significant snowfall. Snow cover has strong seasonality with extensive, but sometimes erratic, winter snow cover and retreat of the snowline to higher elevations during spring and summer and less snow cover. For the upper part of the catchment (upstream of Kyangjin) it has been estimated that snowmelt contributes up to 40% of total runoff (Ragettli et al., 2015).

2.2 Calibration and validation strategy

Remotely sensed snow cover, in situ ~~meteorological~~ observations, and a modified version of the seNorge snow model were combined to estimate SWE and snowmelt runoff dynamics. The remotely sensed snow cover (Landsat 8 and MOD10A2 snow maps) was first validated with in situ snow cover observations provided by surface temperature and snow depth measurements. The snow model was used to simulate daily values of SWE and runoff and was forced by daily in situ meteorological observations of precipitation, temperature and incoming shortwave radiation. MOD10A2 snow cover and snow depth measurements were assimilated to obtain optimal model parameter values using an Ensemble Kalman Filter (EnKF; Evensen, 2003). The optimized parameters were used for a simulation without assimilation of the observations (open-loop). Finally, the model outcome was validated with observed snow depth and Landsat 8 snow cover.

2.3 Datasets

2.3.1 Remotely sensed snow cover

MOD10A2

MOD10A2 is a Moderate Resolution Imaging Spectroradiometer (MODIS) snow cover product available at http://reverb.echo.nasa.gov/. The online sub-setting and reprojection utility was used to clip and project imagery for the Langtang catchment. MOD10A2 provides the 8-day maximum snow extent with a spatial resolution of ~500 m. If there is one snow observation within the 8-day period then the pixel is classified as snow. The 8-day maximum extent offered a good compromise between the temporal resolution and the interference of cloud cover. The snow mapping algorithm used is based on the Normalized Difference Snow Index (NDSI; Hall et al., 1995). The NDSI is a ratio of reflection in short-wave infrared (SWIR) and ~~visible wavelengths~~green light (GREEN) and takes advantage of the properties of snow i.e. snow strongly reflects visible light and strongly absorbs SWIR~~. The NDSI is calculated with spectral bands 4 (0.545-0.565 μm) and 6 (1.628-1.652 μm) following Eq.~~ Eq. (1):

$$NDSI = \frac{\sout{Band\ 4 - Band\ 6}\ GREEN - SWIR}{\sout{Band\ 4 + Band\ 6}\ GREEN + SWIR} \quad (1)$$

The NDSI is calculated with MODIS spectral bands 4 (0.545-0.565 μm) and 6 (1.628-1.652 μm). Pixels are classified as snow when the NDSI ≥ 0.4. Water and dark targets typically have high NDSI values, and to prevent pixels from being incorrectly classified as snow, the reflection should exceed 10% and 11% for spectral bands 2 (0.841-0.876 μm) and 4 respectively for a pixel to be classified as snow (Hall et al., 1995). A full description of the snow mapping algorithm is given by Hall et al. (2002).

Landsat 8

Landsat 8 imagery from 15 April 2013 to 5 November 2014 was downloaded from http://earthexplorer.usgs.gov/. Cloud free scenes~~,~~ (10 out of 34), based on visual inspection, were used to derive daily snow maps with high spatial resolution (30 m). For each image digital numbers were converted to top of atmosphere reflectance. For Landsat 8 the NDSI was calculated with Eq. (1) with spectral bands 3 (0.53-0.59 μm) and 6 (1.57-1.65 μm). The chosen threshold value was equal to that used for the MOD10A2 snow cover product. The NDSI has proven to be a successful snow mapping algorithm for various sensors with a threshold value around 0.4 (Dankers and De Jong, 2004). Although the spectral bands have slightly different band widths and spectral positions, a threshold value of 0.4 gave satisfactory results when compared with in situ snow observations. In addition, the reflection in near-infrared light should exceed 11% to prevent water from being incorrectly classified as snow (Dankers and De Jong, 2004). Therefore, a pixel is classified as snow when the NDSI value ≥ 0.4 and the reflectance in near-infrared light > 11%.

2.3.2 In situ observations

Different types of snow and meteorological observations were available for the study period (January 2013 – September 2014; Table 1, Figure 1). Two transects of surface temperature measurements on a north and south facing slope provided information on snow cover. The 13 temperature sensors (Hobo Tidbits) were positioned on the surface and covered by a small cairn and recorded surface temperature with 10 minute sampling intervals. Snow depths were measured with sonic ranging sensors at 4 locations ~~along the transects~~ at 15 minute intervals. Hourly measurements of snow depth were also made at ~~the~~ Kyangjin and Yala Base Camp automatic weather ~~station~~stations (AWS K and AWS Y; Fig. 1). Hourly means (or totals) of air temperature, liquid and solid precipitation, and incoming shortwave radiation were also recorded at AWS Kyangjin (Shea et al., 2015). Air temperature data was also acquired at several locations with 10 and 15 minute recording intervals.

2.4 Model forcing

The snow model was forced with daily average and maximum air temperature, cumulative precipitation and average incoming shortwave radiation for the time period January 2013 – September 2014. ~~Hourly measurements of air temperature, precipitation and incoming shortwave radiation at AWS Kyangjin were therefore aggregated to daily values. This study period was chosen based on availability of forcing data and observations. Daily temperature lapse rates were interpolated from the air temperature measurements throughout the catchment and used to extrapolate (average and maximum) daily air temperature observed at AWS Kyangjin. The daily observed precipitation and temperature lapse rates were corrected in the modified seNorge snow model with the correction factors $precip$ and T_{tapse} respectively to account for measurement uncertainty (Table 2).~~Hourly measurements of air temperature, precipitation and incoming shortwave radiation at AWS Kyangjin (Shea et al., 2015) were therefore aggregated to daily values. This study period was chosen based on availability of forcing data and observations. Daily temperature lapse rates were interpolated from the air temperature measurements throughout the catchment and used to extrapolate (average and maximum) daily air temperature observed at AWS Kyangjin

(Figure 1). The derived temperature lapse rates agree with the values found by Immerzeel et al. (2014). The daily observed precipitation and temperature lapse rates were corrected in the modified seNorge snow model with the correction factors $precip$ and T_{lapse} respectively to account for the uncertainty related to undercatch and the derived temperature lapse rates (Table 2).

Collier and Immerzeel (2015) modelled the spatial distribution of precipitation in Langtang using an interactively coupled atmosphere and glacier mass balance model (Collier et al., 2013). Their study revealed seasonally contrasting spatial patterns of precipitation within the catchment. Monthly modelled precipitation fields from this study were therefore normalized and used to distribute the observed precipitation at AWS Kyangjin. Similarly, a radiation model (Dam, 2001; Feiken, 2014) was used to extrapolate observed incoming shortwave radiation. The radiation model takes into account the aspect, slope, elevation and shading due to surrounding topography.

The model initial conditions for January 2013 (i.e. SWE and snow depth) were set by simulating year 2013 three times.

2.5 Modified seNorge model

The seNorge snow model (Saloranta, 2012, 2014, 2016) is a temperature-index model which requires only data of air temperature and precipitation. In addition, the seNorge snow model includes a compaction module that can be used to assimilate and validate snow depth rather than snow cover only. The low data requirements and the compaction module make the seNorge snow model suitable for application in this study.

The seNorge snow model was rewritten from its original code into the environmental modelling software PCRaster-Python (Karssenberg et al., 2010) to allow spatio-temporal modelling of the SWE and runoff within the catchment. The snow is modelled as a single homogeneous layer with a spatial resolution of 100 m and a daily time step. The seNorge model was further improved by implementing a different melt algorithm, albedo decay and avalanching. These novel model components are described hereafter and the model parameters used are given in Table 2.

2.5.1 Water balance and snowmelt

Precipitation in the model is partitioned as rain or snow based on an air temperature threshold thr_{snow} (°C). The snowpack consists of a solid component and possibly a liquid component. Meltwater and rain can be stored within the snowpack until its water holding capacity is exceeded and has the possibility to refreeze within the snowpack. The original melt algorithm of the seNorge snow model is substituted by the Enhanced Temperature-Index approach (Pellicciotti et al., 2005, 2008). When air temperature (T; °C) exceeds the temperature threshold for melt onset (TT; °C) the potential melt (M_{pot}; mm d^{-1}) is calculated for each pixel by Eq. (2):

$$M_{pot} = T * TF + SRF * (1 - \alpha) * R_{inc} , \quad (2)$$

where SRF (m^2 mm W^{-2} d^{-1}) is a radiative melt factor, TF (mm $°C^{-1}$ d^{-1}) is a temperature melt factor, α (-) is the albedo of the snow cover and R_{inc} (W m^{-2}) is the incoming shortwave radiation. In case that the threshold temperature is negative, the potential melt can become negative when the radiation melt component is not positive enough to compensate for the negative temperature melt component. When the potential melt is negative it is set to zero to prevent negative values.

The simulated runoff in the seNorge snow model is the total runoff, i.e. the sum of snowmelt and rain. As the focus of this study is on snowmelt runoff it is necessary to split the runoff in snowmelt and rain runoff. Meltwater and rain fill up the snowpack until its water holding capacity is exceeded. The surplus is defined as snowmelt and rain runoff respectively. If both rain and snowmelt occur it is assumed that rain saturates the snowpack first. Rain falling on snow-free portions of the basin is included in the rain runoff totals.

2.5.2 Albedo decay

Decay of the albedo of snow is calculated with the algorithm developed by Brock et al. (2000) in which the albedo is a function of cumulative maximum daily air temperature $T_{\max}$ (°C). When ~~maximum air temperature~~T_{max} is above 0 °C the air temperature is summed as long snow is present and no new snow has fallen. When T_{max} is below 0 °C the albedo remains constant. Albedo decay is calculated differently for deep snow (SWE ≥ 5 mm) and shallow snow (SWE < 5 mm). The albedo decay for deep snow is a logarithmic decay whereas the decay for shallow snow is exponential. This results in a gradual decrease of the albedo for several weeks, which agrees with reality (Brock et al., 2000). When new snow falls the albedo is set to its initial value. In Langtang the observed albedo of fresh snow is 0.84 and the observed minimum precipitation rate to reset the snow albedo is 1 mm d^{-1} (Ragettli et al., 2015).

2.5.3 Avalanching

After snowfall events, avalanching occurs regularly on steep slopes in the catchment. Therefore snow transport due to avalanching is considered to be an important process for redistribution of snow in the Langtang catchment (Ragettli et al., 2015). Snow avalanching is implemented in the model using the SnowSlide algorithm (Bernhardt and Schulz, 2010). For each cell a maximum snow holding depth SWE_{max} (m), depending on slope S (°), is calculated using an exponential regression function following Eq. (3):

$$SWE_{max} = SS_1 + e^{-SS_2 * S}, \quad (3)$$

where SS_1 and SS_2 are empirical coefficients. If SWE exceeds SWE_{max} and the slope exceeds the minimum slope S_{min} for avalanching to occur, then snow is transported to the adjacent downstream cell. Snow can be transported through multiple cells within one time step.

As the snowpack is divided into an ice and liquid component, both the ice and liquid component should be transported downwards. ~~Separate transport and redistribution of both the liquid and ice component is beyond the scope of this study.~~ Avalanches in Langtang catchment mainly occur at high elevations where temperatures are low and (almost) no liquid water is present in the snowpack. It is therefore assumed that avalanches are dry avalanches and that no liquid water is present in the avalanching snow. When there is, in rare circumstances, liquid water present in avalanching snow, the liquid water is converted to the ice component to ensure water balance closure.

2.5.4 Compaction and density

The compaction module is described in detail in Saloranta (2014, 2016). In this module SWE is converted into snow depth. Change in snow depth occurs due to melt, new snow and viscous compaction. The change in snow depth due to new snow is adapted such that an increase in snow depth can occur due to both snowfall and deposition of avalanching snow. The increase in snow depth due to deposition of avalanching snow is calculated using a constant snow density for dry avalanches (200 kg m^{-3}; Hopfinger, 1983).

2.6 Data assimilation

2.6.1 Sensitivity analysis

In order to assess which model parameters to calibrate, a local sensitivity analysis was performed by varying the value of one parameter at a time while holding the values of other parameters fixed. This gives useful first order estimates for parameter sensitivity, although it cannot account for parameter interactions. Plausible parameter values were based on literature (Table 2). The model was run in Monte-Carlo (MC) mode with 100 realizations for each parameter. The values for the parameters were randomly chosen from a uniform distribution with defined minimum and maximum values for the parameters. The snow extent and snow depth were averaged over the study period and study area for the sensitivity analysis. The sensitivity of the modelled mean snow extent and mean snow depth were compared to the changes in parameter values. A pixel is determined to be snow covered in the model when the simulated SWE exceeds 1 mm. All the parameters were varied independently per run, except for the melt factors (TF and SRF) as these are known to be dependent on each other (Ragettli et al., 2015). Therefore, TF and SRF were varied simultaneously in the sensitivity analysis using a linear relation between these melt factors.

2.6.2 Parameter calibration

Using the Ensemble Kalman filter (EnKF; Evensen, 1994) data assimilation of snow extent and snow depth observations was used to calibrate model parameters using the framework developed by Wanders et al. (2013). An advantage of the EnKF calibration framework is that it allows obtaining an uncertainty estimate for the calibrated parameters. The EnKF obtains the simulation uncertainty by using a MC framework, where the spread in the ensemble members represent the combined

uncertainty of parameters and input data. Unfortunately, the EnKF does not allow to reduce and estimate the model structure uncertainty, since it relies on the assumption that the ensemble members are normally distributed. This assumption is no longer valid if multiple model schematizations are used. Therefore, it is assumed that the model is capable to accurately simulate the processes, when provided with the correct parameters. Besides the parameter and model uncertainty there is uncertainty in the observations which are assimilated. The EnKF finds the optimal solution for the model states and parameters, based on the observations and modelled predicted values and their respective uncertainties. With sufficient observations the parameters will convert to a stable solution with an uncertainty estimate that is dependent on the observations error and the ability of the model to simulate the observations. It was found that 50 ensemble members are sufficient to obtain stable parameter solutions and correctly represent the parameter uncertainty.

The EnKF was applied for each time step that observations were available. The MOD10A2 snow extent was divided into 6 elevation zones. The snow extent per elevation zone was derived from the MOD10A2 snow cover and used for assimilation to include more information on spatial distribution of snow. The elevation zone breakpoints are at 3500, 4000, 4500, 5000 and 5500 m asl. Snow maps with more than 30% cloud cover and with obvious miss-classification of snow were exempted from assimilation (3 snow maps out of 88). Only for cloud free pixels comparisons were made between modelled and observed snow extent. Two snow depth observation locations (Pluvio Langshisha and AWS Kyangjin; Figure 1) were also assimilated.

The EnKF framework allows for the inclusion of an uncertainty in the assimilated observations. Point snow depth measurements have high uncertainties that are related to limited representativeness of point snow depth observations in complex terrain due to local influence of snow drift (Grünewald and Lehning, 2015). For the snow depth measurements a variance of 25 cm was chosen to represent the uncertainty of point snow depth measurements. The MOD10A2 snow extent was assigned an uncertainty based on the classification accuracy determined with the in situ snow observations (Sect. 3.1.2 Remotely sensed snow cover). The uncertainty is dependent on the snow extent SE (m^2), i.e. an increase in uncertainty for an increase in snow extent. To prevent the uncertainty to become zero when there is no snow cover, the minimum variance for each zone was restricted to the average snow extent $\overline{SE}_{zone}$ (m^2) times the $accuracy$ (-). Therefore the variance σ^2 per elevation zone is defined following Eq. (4):

$$\sigma^2 = \max((SE_{zone} * accuracy)^2, (\overline{SE}_{zone} * accuracy)^2) \quad (4)$$

The four most sensitive parameters (TT, T_{lapse}, $precip$ and C_6) resulting from the sensitivity analysis were optimized based on the assimilation of snow depth and MOD10A2 snow extent. The first three parameters (TT, T_{lapse} and $precip$) influence both snow depth and snow extent, and were optimized by assimilating MOD10A2 snow extent. The fourth parameter (C_6) only influences snow depth, and was optimized by assimilating snow depth observations and taking into account the full

uncertainty in the previously determined parameters. The two-step approach was chosen to restrict the degrees of freedom and to prevent unrealistic parameter estimates.

2.7 Climate sensitivity

Climate sensitivity tests were performed to investigate changes in SWE and snowmelt runoff as a result of temperature and precipitation changes. Climate sensitivity was tested by perturbing daily average air temperature, daily maximum air temperature and daily cumulative precipitation using a delta-change method. The changes in temperature and precipitation were based on an envelope of projected changes in temperature and precipitation for RCP4.5 for the Langtang catchment as in Immerzeel et al. (2013). Immerzeel et al. (2013) extracted temperature and precipitation trends from all available CMIP5 simulations for the emission scenario RCP 4.5 for Langtang catchment. They selected four models that ranged from dry to wet and from cold to warm. Four climate sensitivity tests were performed ~~ranging from dry to wet and cold to warm~~based on the projected changes found by Immerzeel et al. (2013) (Table 3).

Figure 2 shows the monthly cumulative precipitation and the average daily maximum temperature per month measured at AWS Kyangjin for the study period. This data is also available for the time period 1988-2009 and is used to characterize the climatology of the catchment. Comparison of the measurements of the 1988-2009 period and the study period shows that the maximum temperature is similar for both time periods, whereas more variability exists in the cumulative precipitation. Especially in October a large difference exists in cumulative precipitation, which is caused by a large precipitation event of approximately 100mm during the study period.

3 Results and discussion

3.1 Validation of snow maps with in situ observations

3.1.1 In situ snow observations

Surface temperature is an indirect measure of presence of snow. Figure 3~~Figure 2~~ shows observed surface temperature for two locations. Snow cover is distinguishable based on the low diurnal variability in surface temperature when snow is present due to the isolating effect of snow (Lundquist and Lott, 2008). An optimal threshold for distinguishing between snow/no snow was determined to be 2°C difference between daily minimum temperature and maximum temperature. The use of a larger temperature interval as threshold value was explored, however as diurnal temperature variability is small during monsoon (Immerzeel et al., 2014) setting the diurnal cycle temperature threshold above 2°C may result in incorrect monsoon snow observations.

3.1.2 Remotely sensed snow cover

Both observed surface temperature and snow depth measurements were converted to daily and 8-day maximum binary snow cover values to validate Landsat 8 and MOD10A2 snow cover respectively. We find that the classification accuracy of MOD10A2 and Landsat 8 snow maps based on all in situ snow observations is 83.1% and 85.7% respectively. The classification accuracy is defined as the number of correctly classified pixels divided by the total number of pixels. Table 4 shows the confusion matrices. Misclassification can be a result of variability of snow conditions within a pixel and classification of ice clouds or high cirrus clouds as snow (Parajka and Blöschl, 2006). Large viewing angles, and consequently larger observation areas may also result in misclassification (Dozier et al., 2008). MOD10A2 has a lower spatial resolution than Landsat 8 which likely causes the slightly lower accuracy for the MOD10A2 snow cover product (Hall et al., 2002). Visual inspection of MOD10A2 snow maps also revealed that some clouds are erroneously mapped as snow cover.

The accuracy of MODIS daily snow cover products are reported to be 95% for mountainous Austria (Parajka and Blöschl, 2006) and 94.2% for the Upper Rio Grande Basin (Klein and Barnett, 2003). The lower accuracy presented in this study is likely a result of the simplification of the 8-day composite product and more extreme relief and consequently larger spatial variability in snow cover. Besides classification errors, uncertainty in the in situ snow observations should be considered as well. For the in situ snow cover observations provided by surface temperature there are relatively many observations for which snow is not observed in situ, while the MOD10A2 and Landsat 8 snow maps indicate that snow should be present (Table 5). This may be caused by the fact that a thin snow layer may not result in sufficient isolation to reduce the diurnal temperature fluctuations for observation as snow (Lundquist and Lott, 2008). This observation bias in the temperature-sensed snow cover data would indicate that MOD10A2 and Landsat 8 snow maps possibly have even higher accuracies than presented here based on this validation approach.

3.2 Model calibration

The results of the sensitivity of mean snow extent and mean snow depth to parameter variability are shown in Table 2. The sensitivity analysis shows that the threshold temperature for melt onset (TT), precipitation bias ($precip$), temperature lapse rate bias (T_{lapse}) and the coefficient for conversion for viscosity (C_6) are the most sensitive parameters. For the snow compaction parameters, snow depth is most sensitive for changes in C_6 which is in agreement with Saloranta (2014). The melt parameters SRF and TF influence melt directly but show small sensitivity as these parameters are dependent on each other. A higher value for TF coincides with a lower value for SRF where the value of both parameters is climate zone dependent (Ragettli et al., 2015).

Only the four most sensitive parameters were chosen to be calibrated by the EnKF to limit the degrees of freedom and to prevent the absence of convergence in the solutions for the parameters. Table 6 shows the prior and posterior parameter distribution resulting from the assimilation of snow extent per zone and snow depth. The parameter values for

T_{lapse}, $precip$, and C_6 show a narrow posterior distribution (i.e. small standard deviation) indicating that parameter uncertainty is small. T_{lapse} and ~~$precip$ account for~~$precip$ represent measurement ~~uncertainty~~uncertainties of the model ~~input~~inputs. After calibration the modelled precipitation is increased and the temperature lapse rate is slightly steeper (more negative) than derived. The calibrated value of TT shows a large standard deviation indicating absence of convergence in parameter solutions. This can be either a result of insufficient data to determine the parameter value or insensitivity of the model to the parameter value. A negative value for TT is plausible as melt can occur with air temperatures below 0 °C when incoming shortwave radiation is sufficient. Especially at low latitudes and high elevation, solar radiation is an important cause of snowmelt (Bookhagen and Burbank, 2010). TT is reported to be as negative as -6 °C for Pyramid, Nepalese Himalayas (Pellicciotti et al., 2012). Here TT lies in a range which is even more negative than -6 °C. This is likely to be partly a result of the model structure. When TT is negative the melt algorithm (Eq. (1)) can give negative values. This is prevented by restricting the melt algorithm to a minimum value of zero. This can lead to no melt or refreezing at negative temperatures higher than TT. The restriction makes the algorithm therefore insensitive for very low temperatures and results in absence of convergence in the parameter solutions. The EnKF however does not restrict the parameter values, which allows TT to become too negative.

3.3 Model validation

3.3.1 Snow cover

Both the modelled and MOD10A2 snow extent show strong seasonality of snow cover in the catchment (Figure 4~~Figure 3~~). After calibration modelled snow extent shows notable improvement in elevation zone 3500-4000 m asl during the melt season in 2014. After calibration the threshold temperature for melt onset is lower, resulting in more and earlier onset of snowmelt. Consequently there is a decreased snow extent. The zones in the lower areas are expected to show most improvement as this is the area where snow cover is ephemeral and considerable improvements of the modelled snow extent in elevation zone 3500~~-~~-4000 m asl are indeed observed (Figure 4~~Figure 3~~). The root mean square error (RMSE) decreased from 14.2 to 11.2 km^2 after calibration. The simulated snow extent agrees well with MOD10A2 observed snow cover for the higher elevation zones (>4500 m asl). An exception is the snow extent in summer 2013 in the elevation zone 5000-5500 m asl. The snow model underestimates the snow extent compared to the MOD10A2 snow extent. This discrepancy is possibly the result of i) overestimation of simulated melt, ii) an actual snow event that is simulated as rain by the model due to too high air temperature, or iii) erroneous mapping of clouds as snow in the MOD10A2 snow cover.

The model classification accuracy of snow cover after calibration is 85.9% based on pixel comparison between modelled 8-day maximum snow extent and MOD10A2 snow extent. The classification accuracy is the average classification accuracy over all members. There is only a slight increase of 0.2% in accuracy after calibration, however the performance was already high (85.7%) before calibration. The classification accuracy is lower on ~~slopes in the northern part of the catchment (Figure 4). This area contains~~ steep slopes where avalanching is common, and as the snow extent in avalanching

zones is highly dynamic this is not well captured in the model. Calibration of parameters that influence avalanching might overcome this discrepancy to some degree, however a more advanced approach to avalanche modelling may be required. In addition the spatial resolution of the remotely sensed snow cover is likely to be insufficient to detect the avalanche dynamics. ~~After calibration the accuracy increased in the lower area of the northern slopes which corresponds to the improvement of snow extent in elevation zone 3500-4000 m asl (Figure 4).~~Other potential explanations for lower classification accuracies are uncertainties related to the simulated precipitation phase (rain/snow) and the simulated spatial distribution of precipitation based on Collier and Immerzeel (2015).

Landsat 8 derived snow extent is lower in winter than the modelled snow extent and the MOD10A2 snow extent (Figure 4~~Figure 3~~). Distinct differences between the Landsat 8 instantaneous snow cover observations and the MOD10A2 8-day maximum snow cover extents (Figure 4~~Figure 3~~) can be attributed to (i) the sensitivity of the Landsat 8 snow cover maps to misclassified snow pixels in shaded area, (ii) the much higher spatial resolution of Landsat 8 (Hall et al., 2002) and (iii) the difference between an instantaneous image and an 8-day composite.

The model classification accuracy, based on pixel comparison with Landsat 8 snow maps, increased from 74.7% to 78.2% after calibration. In Table 7 individual model classification accuracy is given based on comparison with each Landsat 8 snow map. Relative low accuracies occur in winter (especially at 20-12-2013 and 05-01-2014) and the model overestimates snow cover compared to the Landsat 8 snow maps (Figure 4~~Figure 3~~). The overestimation of snow cover by the model on 20-12-2013 is particularly large and it can be explained by a small snow event (2.3 mm measured at Kyangjin) a few days before the acquisition~~ day of 2.3 mm measured at Kyangjin. Given the~~. With below zero temperatures the model ~~reveals~~simulates a large snow cover extent, but based on a very small amount. Snow redistribution by wind, a patchy snow cover and/or sublimation may ~~therefore~~also explain the mismatch with the Landsat 8 snow cover in this particular case.

3.3.2 Snow depth

The observed and modelled snow depths at ~~three~~four locations are shown in Figure 5. The simulated snow depth is given for the model simulations i) without calibration, ii) after calibration of snow extent, and iii) after calibration of both snow extent and snow depth. After calibration with snow extent there is an increase in snow depth for Yala pluvio and Yala BC for the entire snow season as result of increased simulated precipitation. For Langshisha and Kyangjin the snow depth mainly decreased after calibration with snow extent. These stations are at a lower elevation, and since the threshold temperature for melt onset is lowered after calibration, this leads to reduced snow depth. At all locations the modelled snow depth decreased after calibration with both snow extent and snow depth due to ~~decrease in the threshold temperature for melt onset after calibration. In addition,~~lowering of the parameter relating snow density to snow depth~~ is lowered after~~. After calibration~~,~~ ~~leading to reduced~~ with both snow extent and snow depth~~. Comparison~~, comparison of modelled and observed snow depth at Langshisha shows good agreement. Especially after calibration the timing of the melt onset during spring is improved. For Yala Pluvio and Yala BC the agreement between modelled and observed snow depth is also good, though improvement of the timing of melt onset is limited. For Kyangjin the modelled snow depth agrees less well with observed snow depth in

spring 2013, but it improves in 2014. In spring the snow cover duration of snow events decreases after calibration and improves the fit with the observed snow depth.

Yala ~~is~~Pluvio and Yala BC are the only ~~location which serves~~locations that serve as an independent validation of snow depth as ~~this station is~~these stations are not used for the assimilation. The simulated melt onset in spring is later compared to what is observed. The diurnal variability of air temperature is high during the pre-monsoon season (March to mid-June; Immerzeel et al., 2014). Though daily average air temperatures are below zero, positive temperatures and snowmelt can occur in the afternoon above 5000 m asl (Shea et al., 2015; Ragettli et al., 2015). This ~~explains~~can explain the difference between simulated and observed melt onset. Using an hourly time step might therefore improve the simulation of snowmelt in spring (Ragettli et al., 2015). While the timing of snowpack depletion at Yala ~~is~~Pluvio and Yala BC are offset from the observations, the modelled quantity of snow is in the same order of magnitude for both modelled and observed time series. Hence there is no substantial overestimation or underestimation of ~~SWE~~snow depth. The RMSE between simulated and observed snow depth decreases after calibration with both snow extent and snow depth compared to the uncalibrated simulation of snow depth and after calibration of only snow extent. This shows the benefit of assimilating both snow extent and snow depth into the snow model to obtain optimal parameter values.

While this study shows an approach in using snow depth observations for assimilation and validation, only ~~three~~four locations with snow depth observations were available. This is insufficient for systematic assimilation and independent validation. However, our approach is useful and is recommended for future studies in the Himalayas in particular when more point observations of snow depth are available.

3.4 ~~Snow processes~~

~~**The snow model contains modules with snow processes such as avalanching, albedo decay**~~**Climate sensitivity of SWE and** ~~**compaction. These processes are shown and discussed in this section.**~~ **snowmelt runoff**

The cumulative basin-wide mean snowfall is 1222 mm for the simulation period. Nearly one-third (31.4~~%~~%) of the snowfall is transported to lower elevations due to avalanching, and 16.2% of the snowfall is transported to elevations lower than 5000 m asl. Transport of snow to lower elevations contributes to snowmelt runoff and has been estimated to be 4.5% of the total water input for the upper part of the Langtang catchment (Ragettli et al., 2015).

~~The simulated compaction and albedo decay at Yala (location of snow depth observation) for an accumulation and ablation period (left and right panel respectively) are shown in Figure 6. During the ablation period, snow depth declines through time while snow density shows an inversed similar trend. Reduction of snow depth is a result of both melt and compaction. A decrease in snow depth on days without melt is a result of viscous compaction i.e. compaction due to weight of overlying snow, which increases the snow density. Increases in snow density are greater on days with snowmelt, as snowmelt influences the viscosity of snow due to presence of liquid water in the snow. When liquid water is present within a snowpack the viscosity of the snowpack decreases and enhances compaction (Vionnet et al., 2012). Therefore the decrease in~~

~~snow depth on days with melt is a result of both compaction and melt. Snow depth increases during the accumulation period due to snowfall. New snow has a lower density than the snowpack and therefore lowers the density of the single layer snowpack. The snow density is for example low in January due to series of snow events, whereas in November a prolonged melt period resulted in a higher snow density.~~

~~At low latitudes and high elevation incoming shortwave radiation is an important cause of snowmelt (Bookhagen and Burbank, 2010). The albedo of snow there has a strong impact on snow melt. For the ablation period the albedo initially decays rapidly (Figure 6). Next the albedo remains constant before the albedo declines again. The albedo decay of snow is modelled as a function of cumulative maximum temperature above 0 °C (Sect. 2.5.2 Albedo decay). The albedo remains constant on days with a maximum air temperature below 0 °C. The rapid decay after snowfall is caused by maximum air temperature above 0 °C and a logarithmic decay function. The logarithmic function also explains the more gradual decay in albedo from 23 November onwards. An initial rapid decrease in albedo after a snow event as well as a more gradual decay over time is characteristic for the decay of albedo (Brock et al., 2000). For the accumulation period the albedo increases occasionally as result of snowfall.~~

~~3.5 Climate sensitivity of SWE and snowmelt runoff~~

The simulation of the SWE for the ~~reference scenario~~ study period shows a pattern of increasing SWE with increasing elevation (Figure 6~~Figure 7~~ and Figure 7). At higher elevation air temperature is lower with more snow accumulation than melt, resulting in a higher gain in SWE over time. The glaciers Langtang and Lansgshisha are positioned at approximately the same elevation (Ragettli et al., 2015), though the SWE is ~~considerable~~considerably higher at Langshisha glacier (Figure 6~~Figure 7). Total precipitation is highest along the southern ridge of the catchment and at high elevation in winter (Collier and Immerzeel, 2015) and therefore explains the difference between the SWE at Langtang and Langshisha glacier.~~) due to the precipitation distribution approach we use. Also, some areas at higher elevation show less SWE than surrounding areas at the same elevation. These areas represent the steep slopes in the catchment where avalanching occurs regularly. The transported snow accumulates below these steep slopes. The snow is transported via single stream paths, resulting in a few pixels with extreme accumulation of SWE. This is mainly visible in the northeastern part of the catchment. Modelling the divergence of transported snow might improve the extreme accumulation simulated for some pixels.

For the climate sensitivity tests a delta-change method is used. This method has limitations as climate variability of future climate is not constant compared to the study period (Kobierska et al., 2013). In addition Kobierska et al. (2013) showed that changes in runoff due to climate change is predicted differently by a physical-based snow model and a parameterized snow model for a glacierized catchment. Parameterized snow models (such as the modified seNorge snow model that is used in this study) are calibrated to fit the current climate and not future climate and might therefore be incapable of predicting future states of the snowpack. However, the scope of this study is to show the sensitivity of the SWE

and snowmelt runoff to changes in air temperature and precipitation, and not a full-fledged climate impact study. Therefore the use of a parameterized snow model and the delta-change method is suitable in this case.

Figure 7 and Figure 8 ~~shows~~show the results of the absolute and relative change in SWE for different climate sensitivity tests. All climate sensitivity tests show a decrease in SWE, but the relative change is greatest at low elevations in the valley. We also observe a strong gradient of decreased ~~SWE~~relative change in SWE with increased elevation. An increase in temperature leads to an increase in melt and more precipitation in form of rain instead of snow. Both processes result in decreased relative change of SWE with elevation. Near the catchment outlet there is an area with 100% decrease in SWE as precipitation will only fall as rain instead of snow.

A slight deviation from the elevational trend in SWE change occurs ~~in elevation zone (~~between 3000~~-~~ and 4000 m asl~~)~~, a zone that could be sensitive to ~~the transition of~~changes in the elevation at which snowfall occurs. The combination of snowfall at higher elevations due to higher temperature and the monthly differing spatial patterns in precipitation are likely to explain the banded patterns.

Changes in SWE and the spatial distribution of SWE will also be affected by changes in total precipitation. The influence of precipitation can be determined based on comparison of the two wet and dry climate sensitivity tests~~.~~ (Figure 7 and Figure 8). A decrease in precipitation results in decreased SWE as there is less snowfall. However, the increased precipitation for the wet/cold and wet/warm climate sensitivity tests (+12.1 and +12.4%, respectively) does not compensate for the temperature-related increase in melt and decrease in snow falling in the valley.

Reduced warming under the wet/cold climate sensitivity test results in a smaller decrease of SWE compared to the wet/warm climate sensitivity test, even in the valley. At higher elevations changes in SWE are weakly negative and in some areas positive. Snowpack sensitivity to temperature change decreases with elevation (Brown and Mote, 2009). ~~The increased SWE under both wet climate sensitivity tests occurs in the southeastern part of the catchment where relatively large amounts of precipitation occur in winter (Collier and Immerzeel, 2015).~~The increased SWE under both wet climate sensitivity tests occurs in the southeastern part of the catchment where relatively large amounts of precipitation occur in winter (Collier and Immerzeel, 2015). The compensating effect of increased precipitation at high elevations is important for glacier systems, and emphasizes the importance of accurate estimations of both change in precipitation and its spatial distribution.

The modelled snowmelt and rain runoff at the catchment outlet is greatest during the monsoon and low during winter (Figure 9). Peak snowmelt and rain runoff occur in June and July respectively. The snowmelt season starts in March when temperatures and insolation are rising, and continues until October. Snowmelt runoff contributes most to total runoff during pre-monsoon and early-monsoon (March-June), which is in agreement with Bookhagen and Burbank (2010). Validation of the simulated runoff with observed runoff was impossible, because (i) there was no reliable runoff data available for the study period as there was no reliable rating curve and (ii) the model focusses on rain and snowmelt runoff, however glacier runoff and delay of runoff due to groundwater and glacier storage is not incorporated in the model structure.

The climate sensitivity of snowmelt and rain runoff is shown in Figure 9. All climate sensitivity tests show an increase in snowmelt runoff from October to May. In contrast, snowmelt runoff decreases from June to September. Higher

temperatures result in more snowmelt and less snowfall during winter and an early melt season which leads to a shift in the peak of snowmelt runoff. Immerzeel et al. (2009) showed that in the upper Indus Basin the peak in snowmelt runoff appears one month earlier by 2071-2100 as result of an increase in temperature and precipitation. However, Immerzeel et al. (2012) showed that total snowmelt runoff remains more or less constant under positive temperature and precipitation trends in the upper part of the Langtang catchment. In their study snowmelt on glaciers is not defined as snowmelt runoff and is therefore a minor component of total runoff, leading to different results.

For the wet climate sensitivity tests total runoff (i.e. the sum of snowmelt and rain runoff) increases throughout the year. The decrease in melt runoff during late melt season is compensated by the increase in rain runoff as there is more precipitation. The future hydrology of the central Himalayas largely depends on precipitation changes as it is dominated by rainfall runoff during the monsoon (Lutz et al., 2014). As we perturb the model with a percentage change in precipitation that is constant through the year, the absolute change in precipitation is greater in the monsoon than in winter. For climate sensitivity tests with decreased precipitation, total runoff from June to September decreases, but from October to May it increases as a result of increased snowmelt. Estimates of seasonal changes in precipitation are thus critical to determine whether rain and snowmelt runoff increases or decreases during monsoon.

4 Conclusions

Remotely sensed snow cover, in situ ~~meteorological~~ observations and a modified seNorge snow model were combined to estimate (climate sensitivity of) SWE and snowmelt runoff in the Langtang catchment. Validation of remotely sensed snow cover (Landsat 8 and MOD10A2 snow maps) show high accuracies (85.7% and 83.1% respectively) against in situ snow observations provided by surface temperature and snow depth measurements. Data assimilation of MOD10A2 snow cover and snow depth measurements using an EnKF proves to be successful for obtaining optimal model parameter values. The applied methodology of simultaneous assimilation of snow cover and snow depth allows for the calibration of important snow parameters and validation of the ~~SWE~~snow depth rather than snow cover alone.~~ -~~ This opens up new possibilities for future snow assessments and sensitivity studies in the Himalayas.

The spatial distribution of SWE averaged over the simulation period (January 2013-September 2014) shows a strong gradient of increasing SWE with increasing elevation. In addition the SWE is considerably higher in the southeastern part of the catchment than the northeastern part of the catchment as a result of the spatial and temporal distribution of precipitation. Climate sensitivity tests show a strong relative decrease in SWE in the valley with increasing temperature due to more snowmelt and less precipitation as snow. At higher elevations an increase in precipitation partly compensates for increased melt due to ~~lower~~higher temperatures. The compensating effect of precipitation emphasizes the importance and need for accurate prediction of change in spatial and temporal distribution of precipitation.

All climate sensitivity tests used in this study show an increase in snowmelt runoff from October to May~~. This is explained by~~, as increased ~~temperature resulting in more~~temperatures will increase snowmelt ~~and less~~, reduce snowfall ~~in~~

~~winter,~~ and lead to an earlier melt season. In contrast, snowmelt totals decrease during the monsoon (June to September) as snow cover and snow depths are reduced. Under wetter ~~scenarios~~climate sensitivity tests, decreased snowmelt in monsoon is partly offset by increased precipitation. This indicates that changes in monsoon intensity and duration will ultimately determine future changes in rainfall and snowmelt totals.

References

Andreadis, K. M. and Lettenmaier, D. P.: Assimilating remotely sensed snow observations into a macroscale hydrology model, , 29, 872–886, doi:10.1016/j.advwatres.2005.08.004, 2006.

Avanzi, F., Michele, C. De, Morin, S., Carmagnola, C. M., Ghezzi, A. and Lejeune, Y.: Model complexity and data requirements in snow hydrology: seeking a balance in practical applications, Hydrol. Process., 30, 2106–2118, doi:10.1002/hyp.10782, 2016.

Barnett, T. P., Adam, J. C. and Lettenmaier, D. P.: Potential impacts of a warming climate on water availability in snow-dominated regions., Nature, 438(7066), 303–309, doi:10.1038/nature04141, 2005.

Barros, A. P., Kim, G., Williams, E. and Nesbitt, S. W.: Probing orographic controls in the Himalayas during the monsoon using satellite imagery, Nat. Hazards Earth Syst. Sci., 4(1), 29–51, 2004.

Bernhardt, M. and Schulz, K.: SnowSlide: A simple routine for calculating gravitational snow transport, Geophys. Res. Lett., 37(11), 1–6, doi:10.1029/2010GL043086, 2010.

Bookhagen, B. and Burbank, D. W.: Toward a complete Himalayan hydrological budget: Spatiotemporal distribution of snowmelt and rainfall and their impact on river discharge, J. Geophys. Res. Earth Surf., 115(3), 1–25, doi:10.1029/2009JF001426, 2010.

Brock, B. W., Willis, I. C. and Sharp, M. J.: Measurement and parameterisation of albedo variations at Haut Glacier d ' Arolla , Switzerland, J. Glaciol., 46(155), 675–688, doi:10.3189/172756506781828746, 2000.

Brown, R. D. and Mote, P. W.: The response of Northern Hemisphere snow cover to a changing climate*, J. Clim., 22(8), 2124–2145, doi:10.1175/2008JCLI2665.1, 2009.

Clark, M. P., Slater, A. G., Barrett, A. P., Hay, L. E., Mccabe, G. J., Rajagopalan, B. and Leavesley, G. H.: Assimilation of snow covered area information into hydrologic and land-surface models and land-surface models, Adv. Water Resour., 29, 1209–1221, doi:10.1016/j.advwatres.2005.10.001, 2006.

Collier, E. and Immerzeel, W. W.: High-resolution modeling of atmospheric dynamics in the Nepalese ~~H~~Himalaya, J. Geophys. Res. Atmos., 120(19), 9882–9896, doi:10.1002/2015JD023266.Received, 2015.

Collier, E., Mölg, T., Maussion, F., Scherer, D., Mayer, C. and Bush, A. B. G.: High-resolution interactive modelling of the mountain glacier-atmosphere interface: An application over the Karakoram, Cryosphere, 7(3), 779–795, doi:10.5194/tc-7-779-2013, 2013.

Dam, O. Van: Forest filled with gaps: effects of gap size on water and nutrient cycling in tropical rain forest: a study in

Guyana. [online] Available from: http://igitur-archive.library.uu.nl/dissertations/1954687/title.pdf, 2001.

Dankers, R. and De Jong, S.: Monitoring snow-cover dynamics in Northern Fennoscandia with SPOT VEGETATION images, Int. J. Remote Sens., 25(15), 2933–2949, doi:10.1080/01431160310001618374, 2004.

Dong, J., Walker, J. P. and Houser, P. R.: Factors affecting remotely sensed snow water equivalent uncertainty, Remote Sens. Environ., 97(1), 68–82, doi:10.1016/j.rse.2005.04.010, 2005.

Dozier, J., Painter, T. H., Rittger, K. and Frew, J. E.: Time – space continuity of daily maps of fractional snow cover and albedo from MODIS, Adv. Water Resour., 31(11), 1515–1526, doi:10.1016/j.advwatres.2008.08.011, 2008.

Durand, M., Molotch, N. P. and Margulis, S. A.: Merging complementary remote sensing datasets in the context of snow water equivalent reconstruction, Remote Sens. Environ., 112, 1212–1225, doi:10.1016/j.rse.2007.08.010, 2008.

Evensen, G.: Sequential data assimilation with a nonlinear quasi-geostrophic model using Monte Carlo methods to forecast error statistics, J. Geophys. Res., 99(C5), 143–162, 1994.

Evensen, G.: The Ensemble Kalman Filter : theoretical formulation and practical implementation, Ocean Dyn., 53, 343–367, doi:10.1007/s10236-003-0036-9, 2003.

Feiken, H.: Dealing with biases: three archaeological approaches to the hidden landscapes of Italy, Barkhuis; Groningen University Library., 2014.

Grünewald, T. and Lehning, M.: Are flat-field snow depth measurements representative? A comparison of selected index sites with areal snow depth measurements at the small catchment scale, Hydrol. Process., 29(7), 1717–1728, doi:10.1002/hyp.10295, 2015.

Gurung, D. R., Kulkarni, A. V., Giriraj, A., Aung, K. S., Shrestha, B. and Srinivasan, J.: Changes in seasonal snow cover in Hindu Kush-Himalayan region, Cryosph. Discuss., 5(2), 755–777, doi:10.5194/tcd-5-755-2011, 2011.

Hall, D. K., Riggs, G. a and Salomonson, V. V: Development of methods for mapping global snow cover using moderate resolution imaging spectroradiometer data, Remote Sens. Environ., 54(2), 127–140, doi:10.1016/0034-4257(95)00137-P, 1995.

Hall, D. K., Riggs, G. A., Salomonson, V. V., DiGirolamo, N. E. and Bayr, K. J.: MODIS snow-cover products, Remote Sens. Environ., 83(1–2), 181–194, doi:10.1016/S0034-4257(02)00095-0, 2002.

Hopfinger, E. J.: Snow Avalanche Motion and Related Phenomena, Annu. Rev. Fluid Mech., 15, 47–76, doi:10.1146/annurev.fl.15.010183.000403, 1983.

Immerzeel, W. W., Droogers, P., de Jong, S. M. and Bierkens, M. F. P.: Large-scale monitoring of snow cover and runoff simulation in Himalayan river basins using remote sensing, Remote Sens. Environ., 113(1), 40–49, doi:10.1016/j.rse.2008.08.010, 2009.

Immerzeel, W. W., van Beek, L. P. H. and Bierkens, M. F. P.: Climate change will affect the Asian water towers., Science (80-.)., 328(5984), 1382–5, doi:10.1126/science.1183188, 2010.

Immerzeel, W. W., van Beek, L. P. H., Konz, M., Shrestha, A. B. and Bierkens, M. F. P.: Hydrological response to climate change in a glacierized catchment in the Himalayas, Clim. Change, 110(3–4), 721–736, doi:10.1007/s10584-011-0143-4,

2012.

Immerzeel, W. W., Pellicciotti, F. and Bierkens, M. F. P.: Rising river flows throughout the twenty-first century in two Himalayan glacierized watersheds, Nat. Geosci., 6(9), 742–745, doi:10.1038/ngeo1896, 2013.

Immerzeel, W. W., Petersen, L., Ragettli, S. and Pellicciotti, F.: The importance of observed gradients of air temperature and precipitation for modeling runoff ~~froma glacierized watershed The importance of observed gradients of air temperature and precipitation for modeling runoff froma~~from a glacierized watershed in the ~~Nepa~~Nepalese Himalaya, Water Resour. Res., 50, 2212–2226, doi:10.1002/2013WR014506~~. Received~~, 2014.

Karssenberg, D., Schmitz, O., Salamon, P., de Jong, K. and Bierkens, M. F. P.: A software framework for construction of process-based stochastic spatio-temporal models and data assimilation, Environ. Model. Softw., 25(4), 489–502, doi:10.1016/j.envsoft.2009.10.004, 2010.

Klein, A. G. and Barnett, A. C.: Validation of daily MODIS snow cover maps of the Upper Rio Grande River Basin for the 2000-2001 snow year, Remote Sens. Environ., 86(2), 162–176, doi:10.1016/S0034-4257(03)00097-X, 2003.

Kobierska, F., Jonas, T., Zappa, M., Bavay, M., Magnusson, J. and Bernasconi, S. M.: Future runoff from a partly glacierized watershed in Central Switzerland : A two-model approach, Adv. Water Resour., 55, 204–214, doi:10.1016/j.advwatres.2012.07.024, 2013.

Leisenring, M. and Moradkhani, H.: Snow water equivalent prediction using Bayesian data assimilation methods, Stoch. Environ. Res. Risk Assess., 25(2), 253–270, doi:10.1007/s00477-010-0445-5, 2011.

Liu, Y., Peters-Lidard, C. D., Kumar, S., Foster, J. L., Shaw, M., Tian, Y. and Fall, G. M.: Assimilating satellite-based snow depth and snow cover products for improving snow predictions in Alaska, Adv. Water Resour., 54, 208–227, doi:10.1016/j.advwatres.2013.02.005, 2013.

Lundquist, J. D. and Lott, F.: Using inexpensive temperature sensors to monitor the duration and heterogeneity of snow-covered areas, Water Resour. Res., 44(4), doi:10.1029/2008WR007035, 2008.

Lutz, A. F., Immerzeel, W. W., Litt, M., Bajracharya, S. and Shrestha, A. B.: Comprehensive Review of Climate Change and the Impacts on Cryosphere, Hydrological Regimes and Glacier Lakes., 2015.

Lutz, a. F., Immerzeel, W. W., Shrestha, a. B. and Bierkens, M. F. P.: Consistent increase in High Asia's runoff due to increasing glacier melt and precipitation, Nat. Clim. Chang., 4(7), 587–592, doi:10.1038/nclimate2237, 2014.

Magnusson, J., Farinotti, D., Jonas, T. and Bavay, M.: Quantitative evaluation of different hydrological modelling approaches in a partly glacierized Swiss watershed, Hydrol. Process., 25(13), 2071–2084, doi:10.1002/hyp.7958, 2011.

Magnusson, J., Wever, N., Essery, R., Helbig, N., Winstral, A. and Jonas, T.: Evaluating snow models with varying process representations for hydrological applications: Snow model evaluation, Water Resour. Res., 51(4), 2707–2723, doi:10.1002/2014WR016498, 2015.

Maskey, S., Uhlenbrook, S. and Ojha, S.: An analysis of snow cover changes in the Himalayan region using MODIS snow products and in-situ temperature data, Clim. Change, 108(1), 391–400, doi:10.1007/s10584-011-0181-y, 2011.

Molotch, N. P.: Reconstructing snow water equivalent in the Rio Grande headwaters using remotely sensed snow cover data

and a spatially distributed snowmelt model, Hydrol. Process., 23, 1076–1089, doi:10.1002/hyp.7206, 2009.

Molotch, N. P. and Margulis, S. A.: Estimating the distribution of snow water equivalent using remotely sensed snow cover data and a spatially distributed snowmelt model: A multi-resolution, multi-sensor comparison, Adv. Water Resour., 31(11), 1503–1514, doi:10.1016/j.advwatres.2008.07.017, 2008.

Nagler, T., Rott, H., Malcher, P. and Müller, F.: Assimilation of meteorological and remote sensing data for snowmelt runoff forecasting, Remote Sens. Environ., 112, 1408–1420, doi:10.1016/j.rse.2007.07.006, 2008.

Parajka, J. and Blöschl, G.: Validation of MODIS snow cover images over Austria, Hydrol. Earth Syst. Sci. Discuss., 3(4), 1569–1601, doi:10.5194/hessd-3-1569-2006, 2006.

Pellicciotti, F., Brock, B., Strasser, U., Burlando, P., Funk, M. and Corripio, J.: An enhanced temperature-index glacier melt model including the shortwave radiation balance: Development and testing for Haut Glacier d'Arolla, Switzerland, J. Glaciol., 51(175), 573–587, doi:10.3189/172756505781829124, 2005.

Pellicciotti, F., Helbing, J., Rivera, A., Favier, V., Corripio, J., Araos, J., Sicart, J. E. and Carenzo, M.: A study of the energy balance and melt regime on Juncal Norte Glacier, semi-arid Andes of central Chile, using melt models of different complexity, Hydrol. Process., 22(19), 3980–3997, doi:10.1002/hyp.7085, 2008.

Pellicciotti, F., Buergi, C., Immerzeel, W. W., Konz, M. and Shrestha, A. B.: Challenges and Uncertainties in Hydrological Modeling of Remote Hindu Kush–Karakoram–Himalayan (HKH) Basins: Suggestions for Calibration Strategies, Mt. Res. Dev., 32, 39–50, doi:10.1659/MRD-JOURNAL-D-11-00092.1, 2012.

Putkonen, J. K.: Continuous Snow and Rain Data at 500 to 4400 m Altitude near Annapurna, Nepal, 1999-2001, Arctic, Antarct. Alp. Res., 36(2), 244–248, 2004.

Ragettli, S., Pellicciotti, F., Bordoy, R. and Immerzeel, W. W.: Sources of uncertainty in modeling the glaciohydrological response of a Karakoram watershed to climate change, Water Resour. Res., 49(9), 6048–6066, doi:10.1002/wrcr.20450, 2013.

Ragettli, S., Pellicciotti, F., Immerzeel, W. W., Miles, E. S., Petersen, L., Heynen, M., Shea, J. M., Stumm, D., Joshi, S. and Shrestha, A.: Unraveling the hydrology of a Himalayan catchment through integration of high resolution in situ data and remote sensing with an advanced simulation model, Adv. Water Resour., 78, 94–111, doi:10.1016/j.advwatres.2015.01.013, 2015.

Saloranta, T. M.: Simulating snow maps for Norway: Description and statistical evaluation of the seNorge snow model, Cryosphere, 6(6), 1323–1337, doi:10.5194/tc-6-1323-2012, 2012.

Saloranta, T. M.: Simulating more accurate snow maps for Norway with MCMC parameter estimation method, Cryosph. Discuss., 8(2), 1973–2003, doi:10.5194/tcd-8-1973-2014, 2014.

Saloranta, T. M.: Operational snow mapping with simplified data assimilation using the seNorge snow model, J. Hydrol., 538, 314–325, doi:10.1016/j.jhydrol.2016.03.061, 2016.

Shea, J. M., Wagnon, P., Immerzeel, W. W., Biron, R., Brun, F., Pellicciotti, F., Wagnon, P., Immerzeel, W. W., Biron, R., Brun, F. and Pellicciotti, F.: A comparative high-altitude meteorological analysis from three catchments in the Nepalese

Himalaya, , 31(2), 174–200, doi:10.1080/07900627.2015.1020417, 2015.

Tahir, A. A., Chevallier, P., Arnaud, Y. and Ahmad, B.: Snow cover dynamics and hydrological regime of the Hunza River basin, Karakoram Range, Northern Pakistan, Hydrol. Earth Syst. Sci., 15(7), 2275–2290, doi:10.5194/hess-15-2275-2011, 2011.

~~Vionnet, V., Brun, E., Morin, S., Boone, A., Faroux, S., Le Moigne, P., Martin, E. and Willemet, J. M.: The detailed snowpack scheme Crocus and its implementation in SURFEX v7.2, Geosci. Model Dev., 5(3), 773–791, doi:10.5194/gmd-5-773-2012, 2012.~~

Wanders, N., De Jong, S. M., Roo, A., Bierkens, M. F. P. and Karssenberg, D.: The benefits of using remotely sensed soil moisture in parameter identification of large-scale hydrological models, Water Resour. Res., 50, 6874–6891, doi:10.1002/2013WR014639, 2013.

Warscher, M., Strasser, U., Kraller, G., Marke, T., Franz, H. and Kunstmann, H.: Performance of complex snow cover descriptions in a distributed hydrological model system: A case study for the high Alpine terrain of the Berchtesgaden Alps, Water Resour. Res., 49, 2619–2637, doi:10.1002/wrcr.20219, 2013.

Wulf, H., Bookhagen, B. and Scherler, D.: Differentiating between rain, snow, and glacier contributions to river discharge in the western Himalaya using remote-sensing data and distributed hydrological modeling, Adv. Water Resour., 88, 152–169, doi:10.1016/j.advwatres.2015.12.004, 2016.

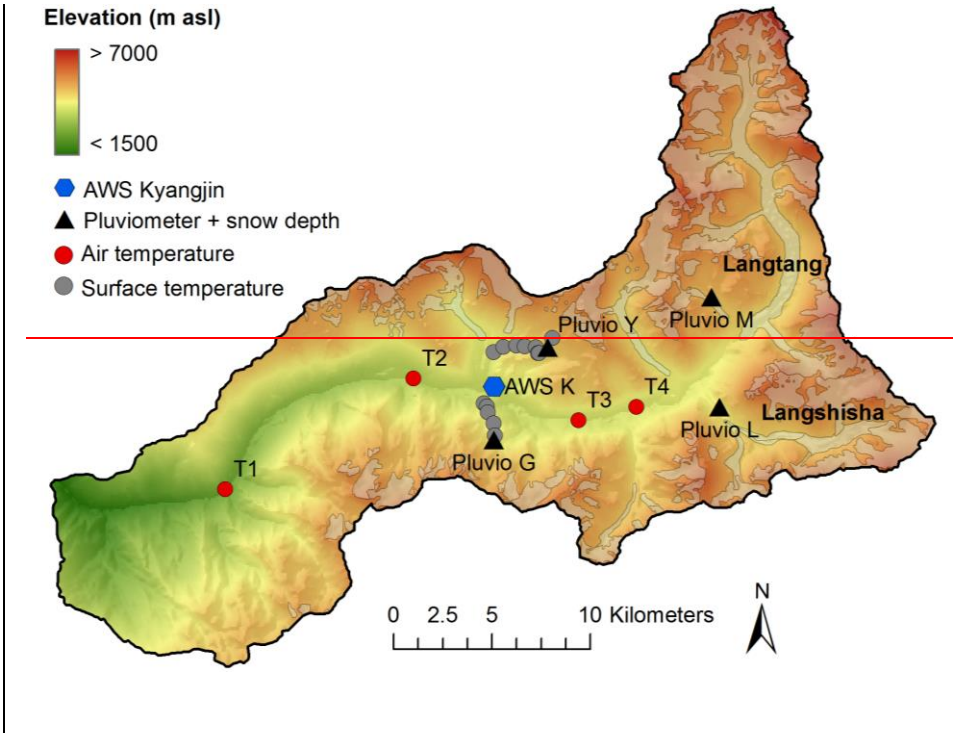
Elevation (m asl)
> 7000
< 1500
AWS Kyangjin
Pluviometer + snow depth
Air temperature
Surface temperature
Langtang
Pluvio Y
Pluvio M
T2
AWS K
T3
T4
Langshisha
Pluvio L
Pluvio G
T1
0 2.5 5 10 Kilometers
N

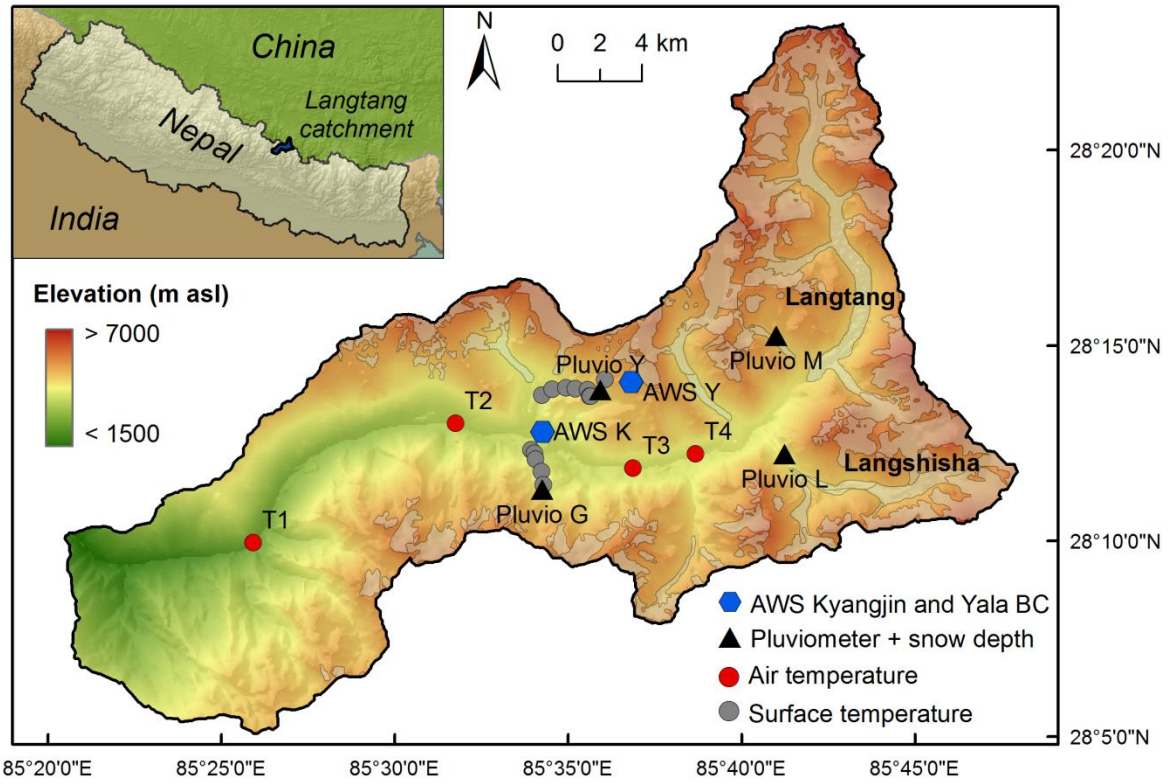

Figure 1: Study area with the locations of the in situ observations. Langtang and Langshisha refer to the two main glaciers in the upper Langtang valley.

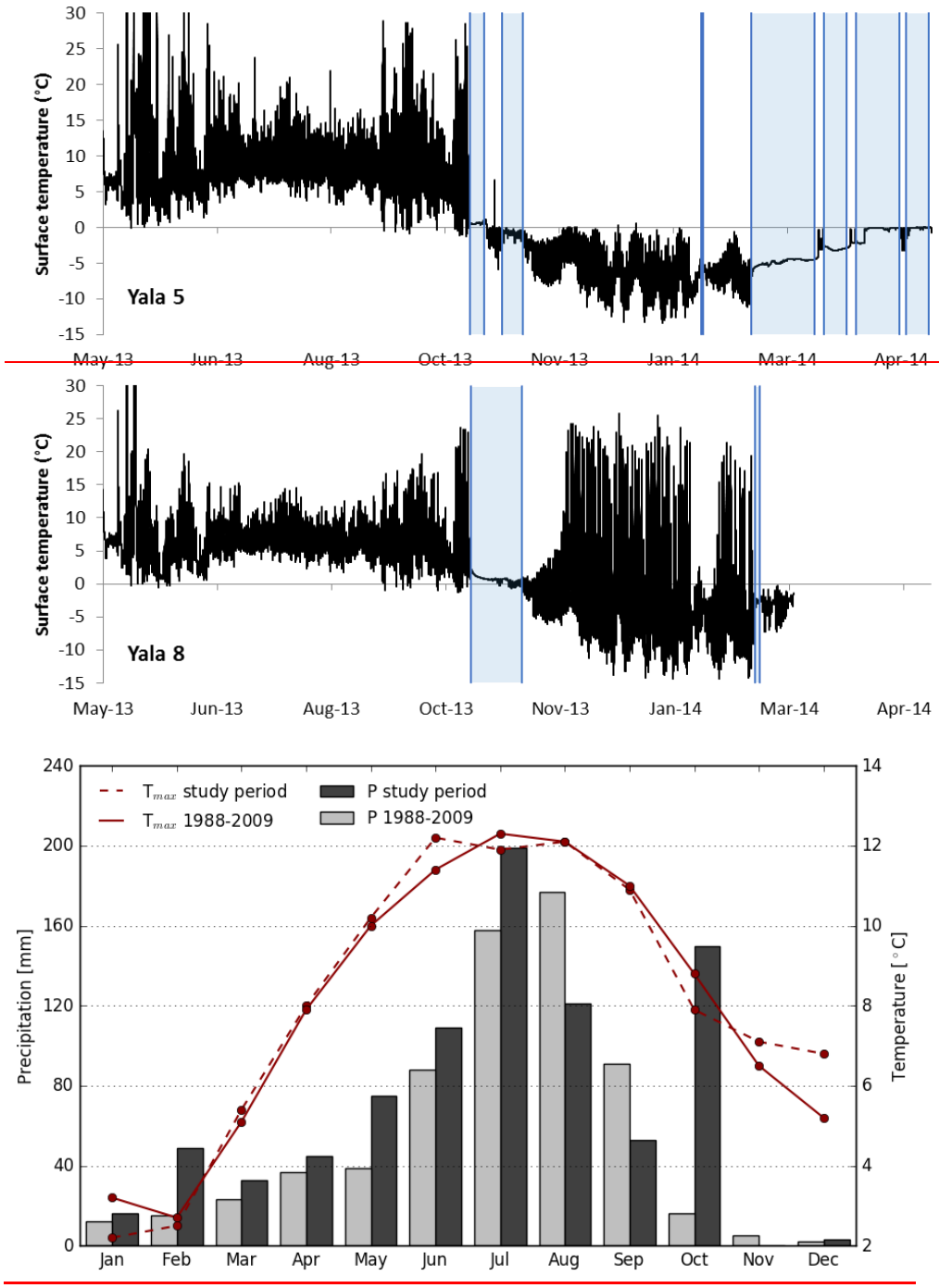

Figure 2 Comparison of maximum temperature (T_{max}) and cumulative monthly precipitation (P) for the study period (January 2013-September 2014) and the 1988-2009 time series (based on measurements in Kyangjin). The average yearly cumulative precipitation is 853mm and 663mm for the study period and the 1988-2009 time series respectively.

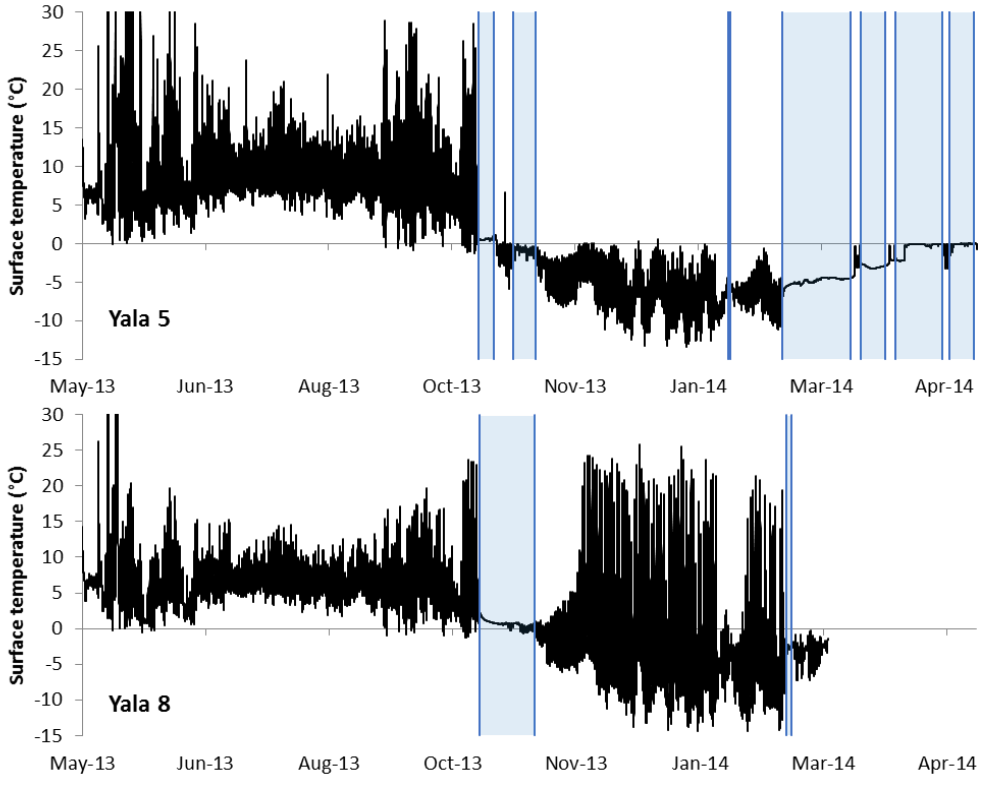

Figure 3: Observed surface temperature with 10 minute interval at two locations. (Table 1). The blue vertical lines indicate the start and end of the snow cover.

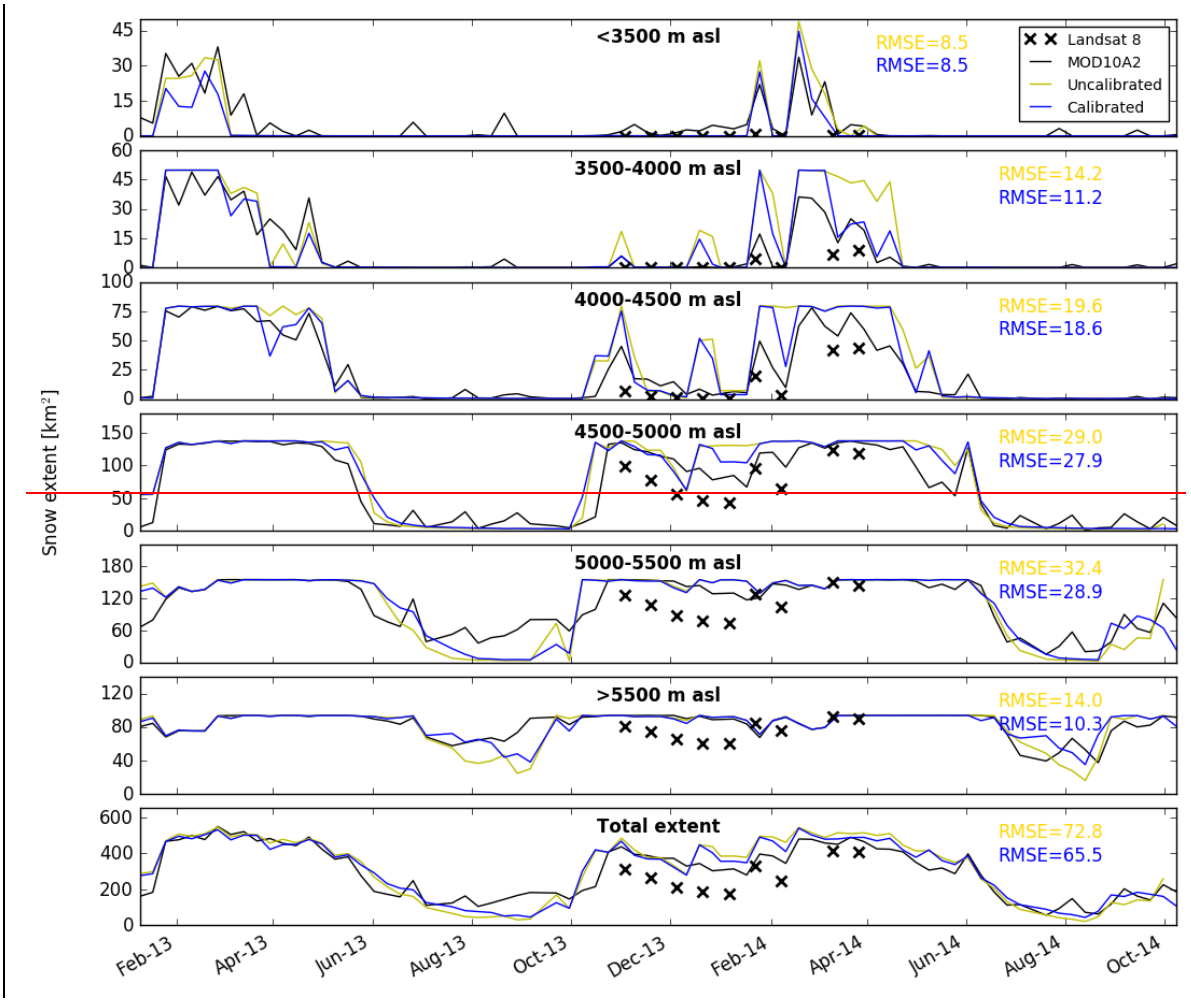
<3500 m asl
RMSE=8.5
RMSE=8.5
Landsat 8
MOD10A2
Uncalibrated
Calibrated
3500-4000 m asl
RMSE=14.2
RMSE=11.2
4000-4500 m asl
RMSE=19.6
RMSE=18.6
4500-5000 m asl
RMSE=29.0
RMSE=27.9
5000-5500 m asl
RMSE=32.4
RMSE=28.9
>5500 m asl
RMSE=14.0
RMSE=10.3
Total extent
RMSE=72.8
RMSE=65.5
Snow extent [km²]
Feb-13
Apr-13
Jun-13
Aug-13
Oct-13
Dec-13
Feb-14
Apr-14
Jun-14
Aug-14
Oct-14

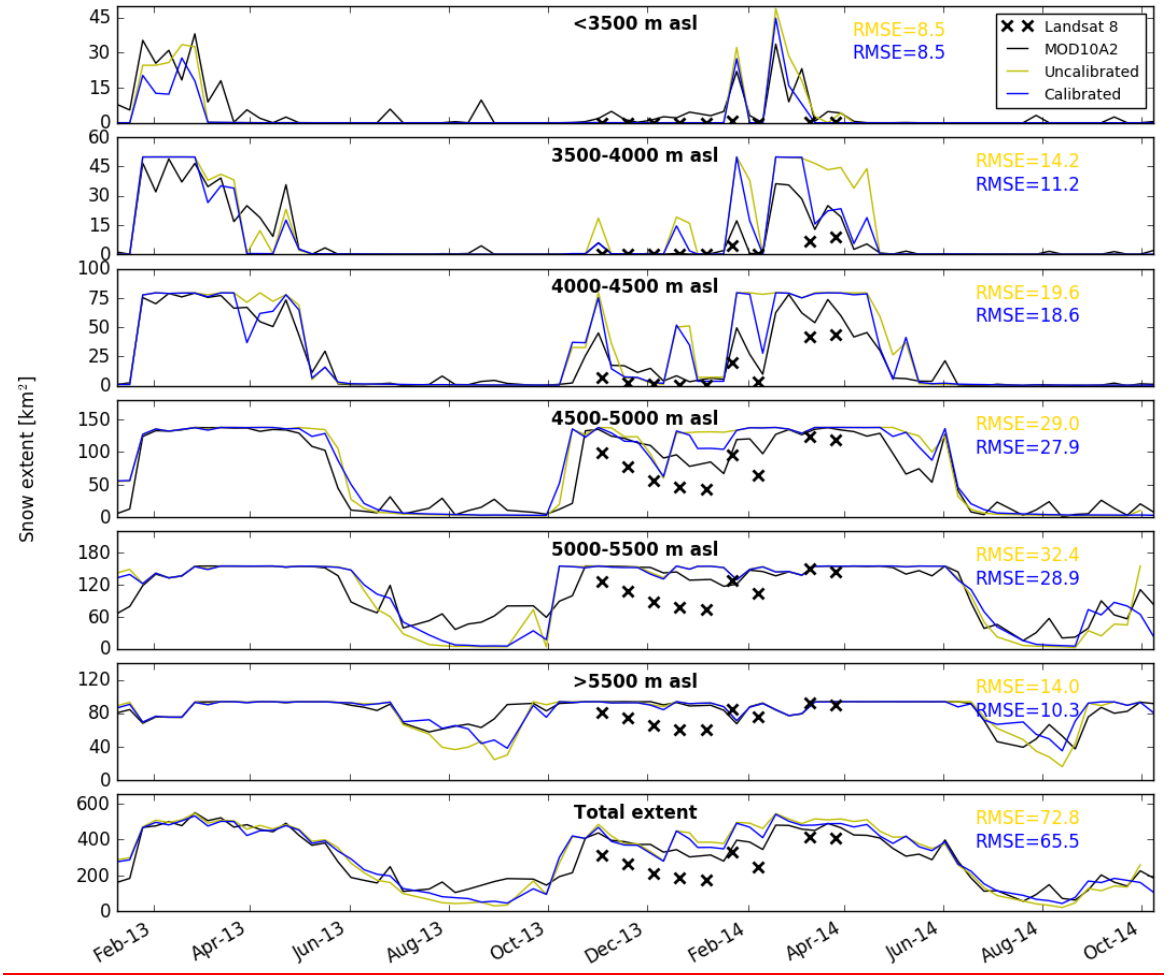

Figure 4~~3~~: Modelled 8-day maximum snow extent before and after calibration (ensemble mean), Landsat 8 snow extent and MOD10A2 snow extent per elevation zone. The RMSE (km^2) is given per zone for the fit between modelled (before and after calibration) and MOD10A2 snow extent.

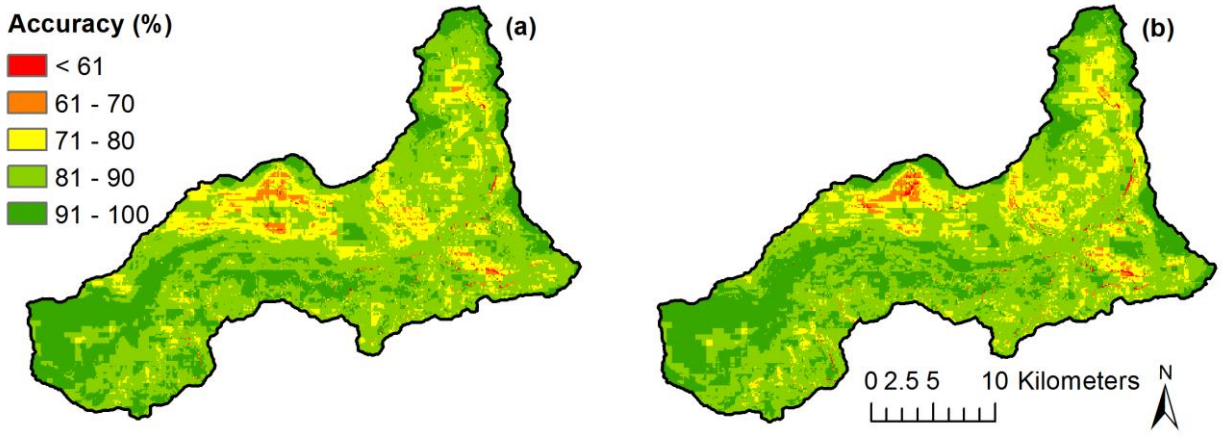

~~**Figure 4: Accuracy per pixel based on comparison between MOD10A2 snow extent and modelled 8-day maximum snow extent a) before calibration and b) after calibration.**~~

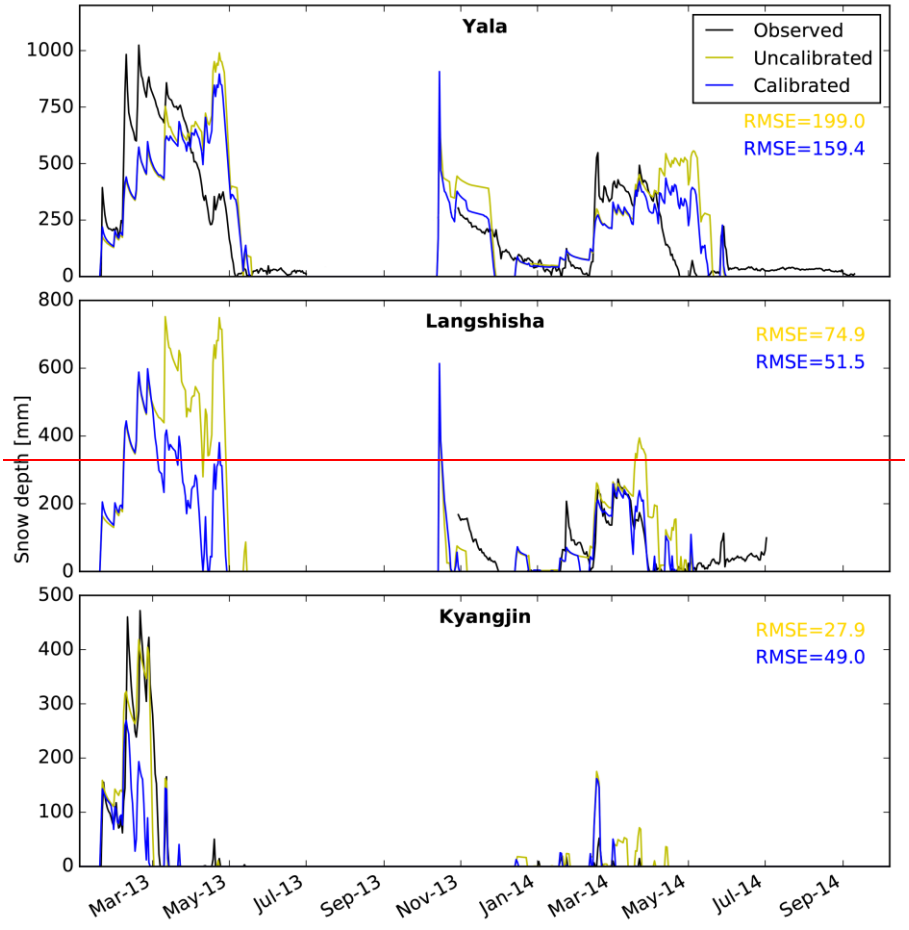

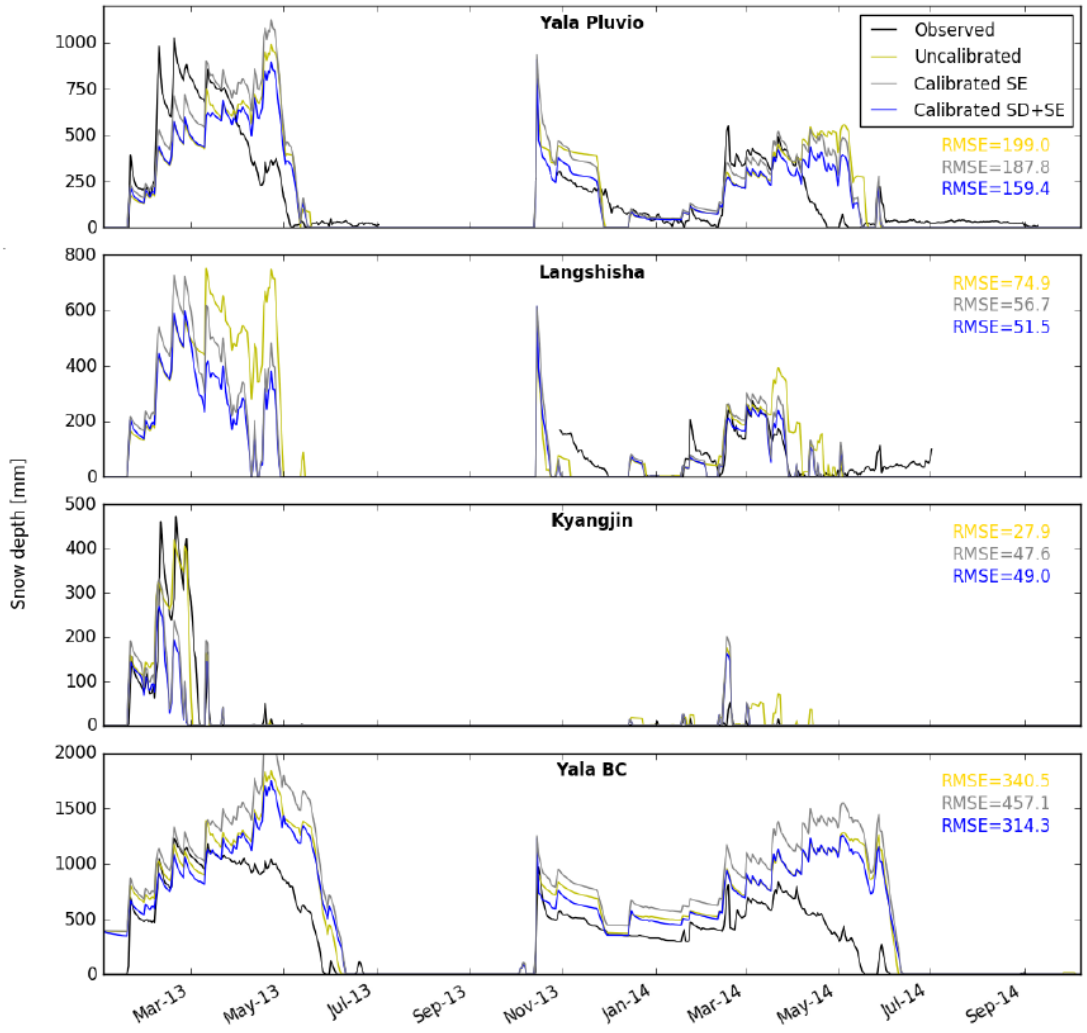

Figure 5: Observed snow depth and modelled snow depth i) before calibration, ii) after calibration of snow extent (SE), and iii) after calibration of both snow extent and snow depth (SD+SE) (ensemble mean) at three locations. The RMSE (mm) is given for the fit between modelled (before and after calibration) and observed snow depth.

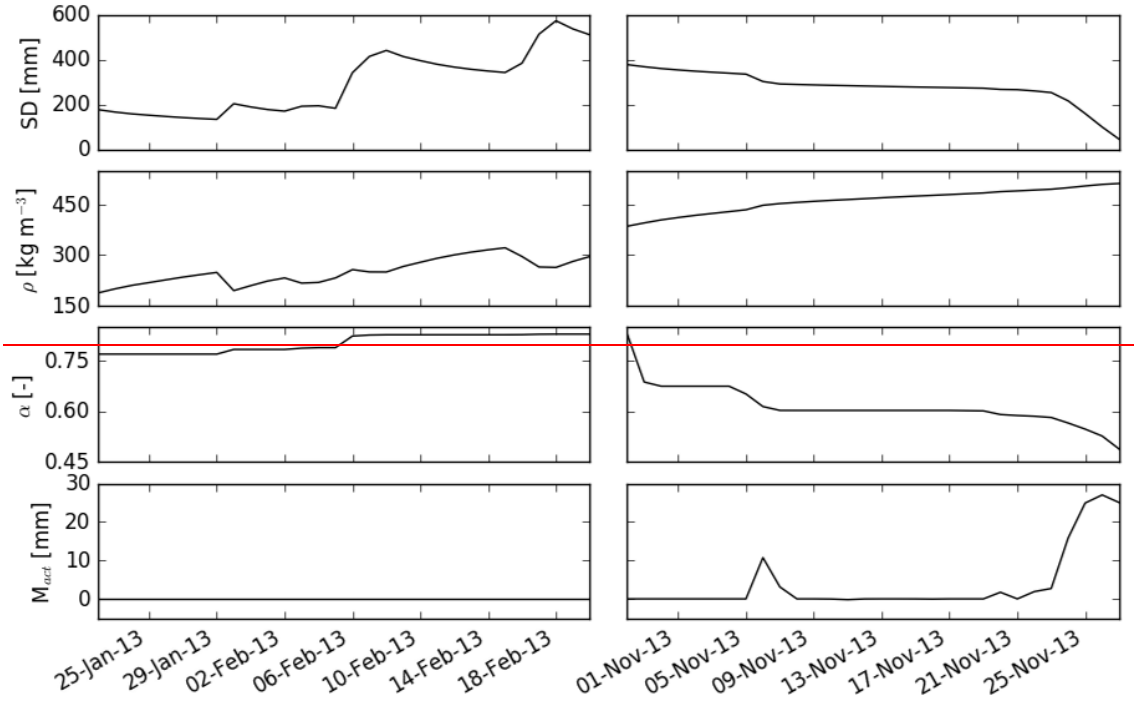

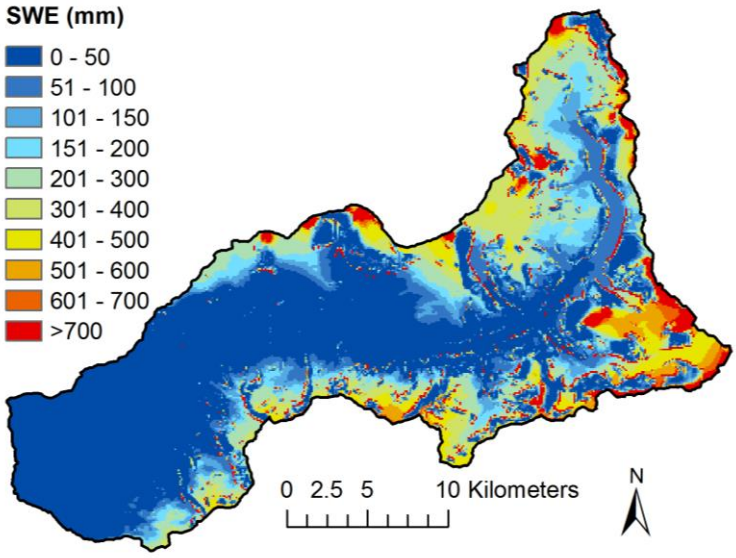

Figure 6: ~~Snow processes at Yala. SD is the snow depth, ρ is the density, α is the albedo of the snow cover, M_{act} is the actual snowmelt. The plotted variables represent the ensemble mean.~~

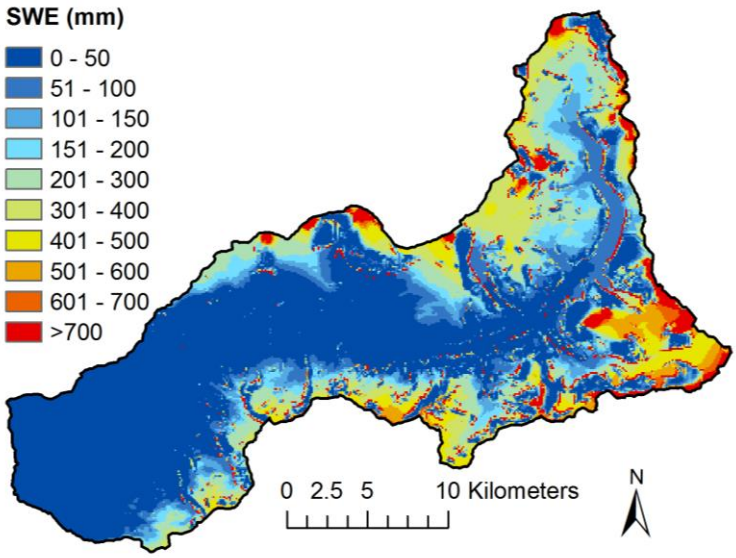

~~Figure 7:~~ Spatial distribution of ensemble mean annual average snow water equivalent (SWE).

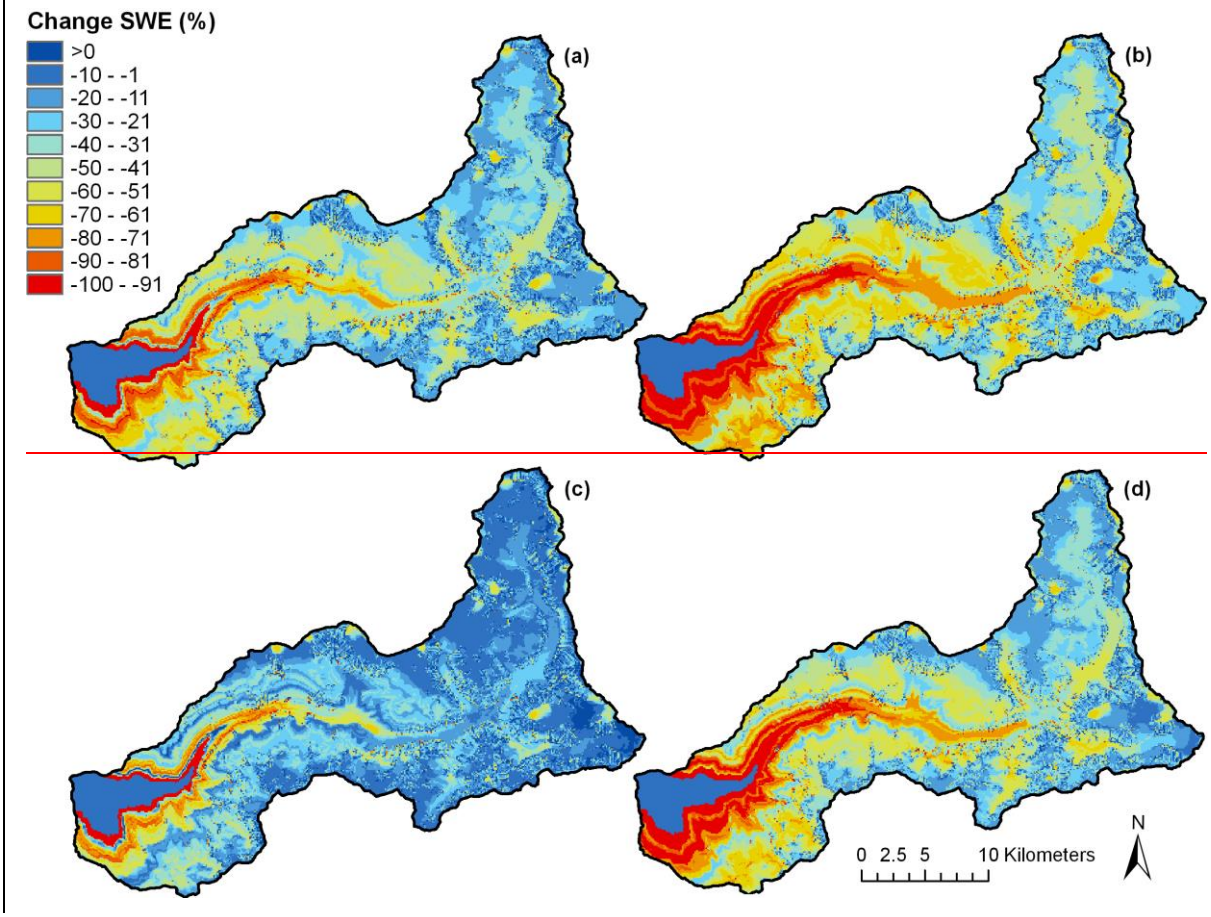
Change SWE (%)
>0
-10 - -1
-20 - -11
-30 - -21
-40 - -31
-50 - -41
-60 - -51
-70 - -61
-80 - -71
-90 - -81
-100 - -91
(a)
(b)
(c)
(d)
0 2.5 5 10 Kilometers
N

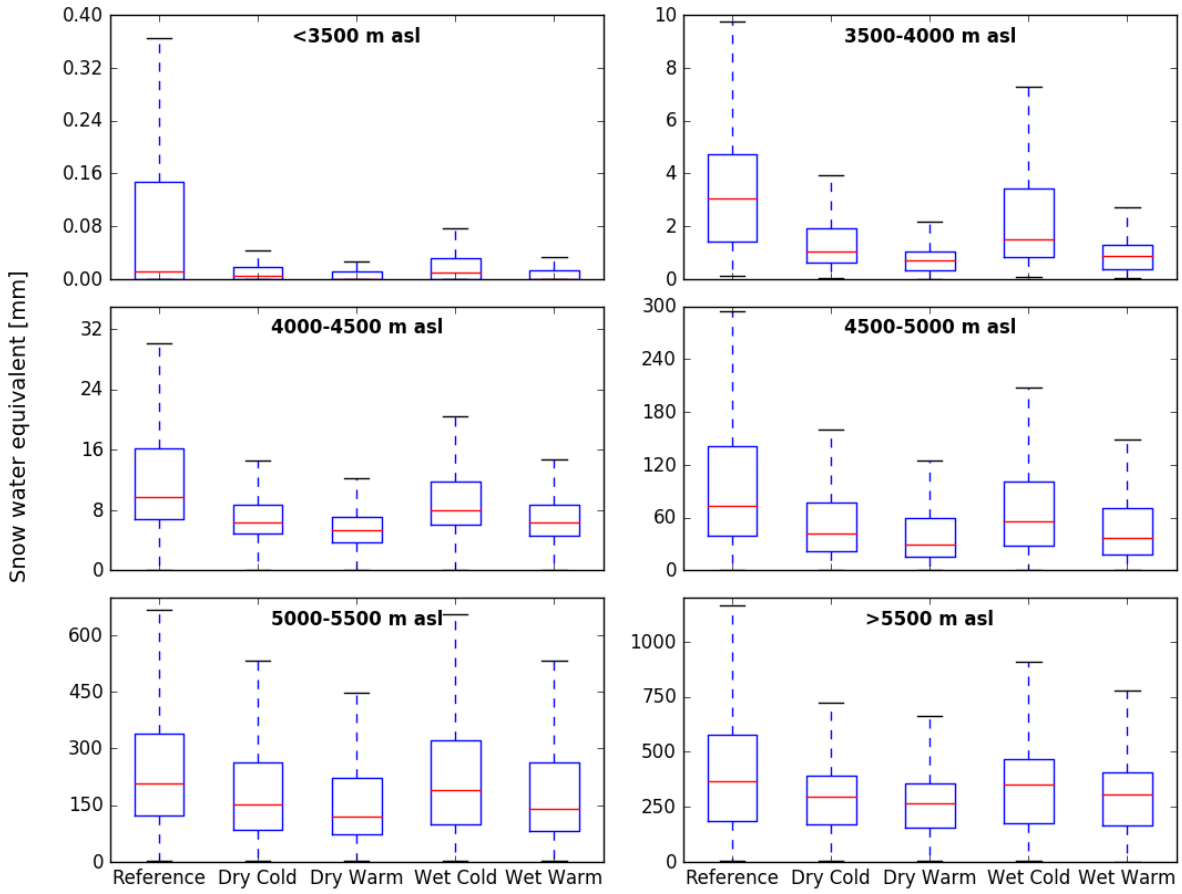

Figure 7 Boxplots of SWE per elevation zone averaged over the simulation period and all ensemble members for the study period (reference) and the four climate sensitivity tests (Table 3).

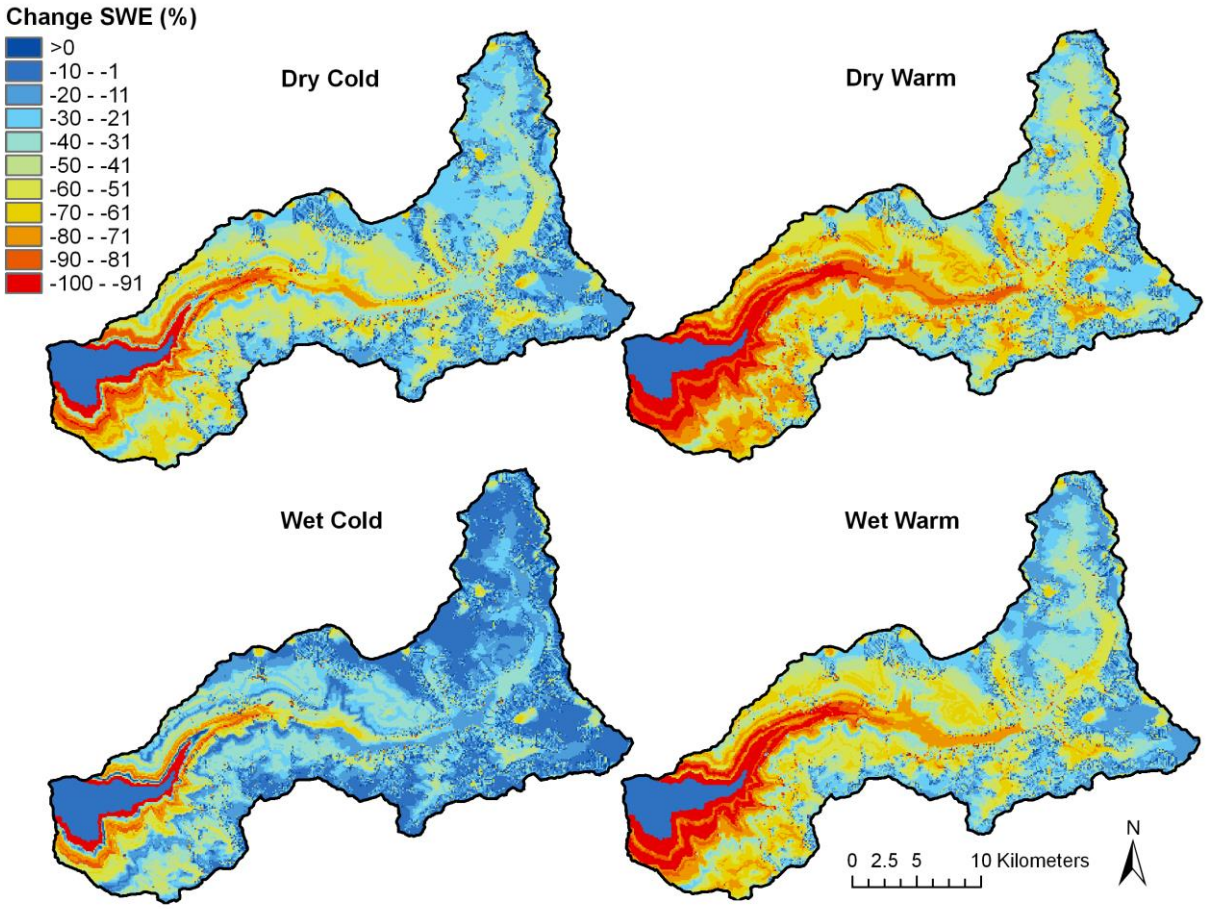

Figure 8: Change in SWE averaged over the simulation period and all members for each climate sensitivity test~~: a) dry and cold b) dry and warm c) wet and cold d) wet and warm.~~ (Table 3).

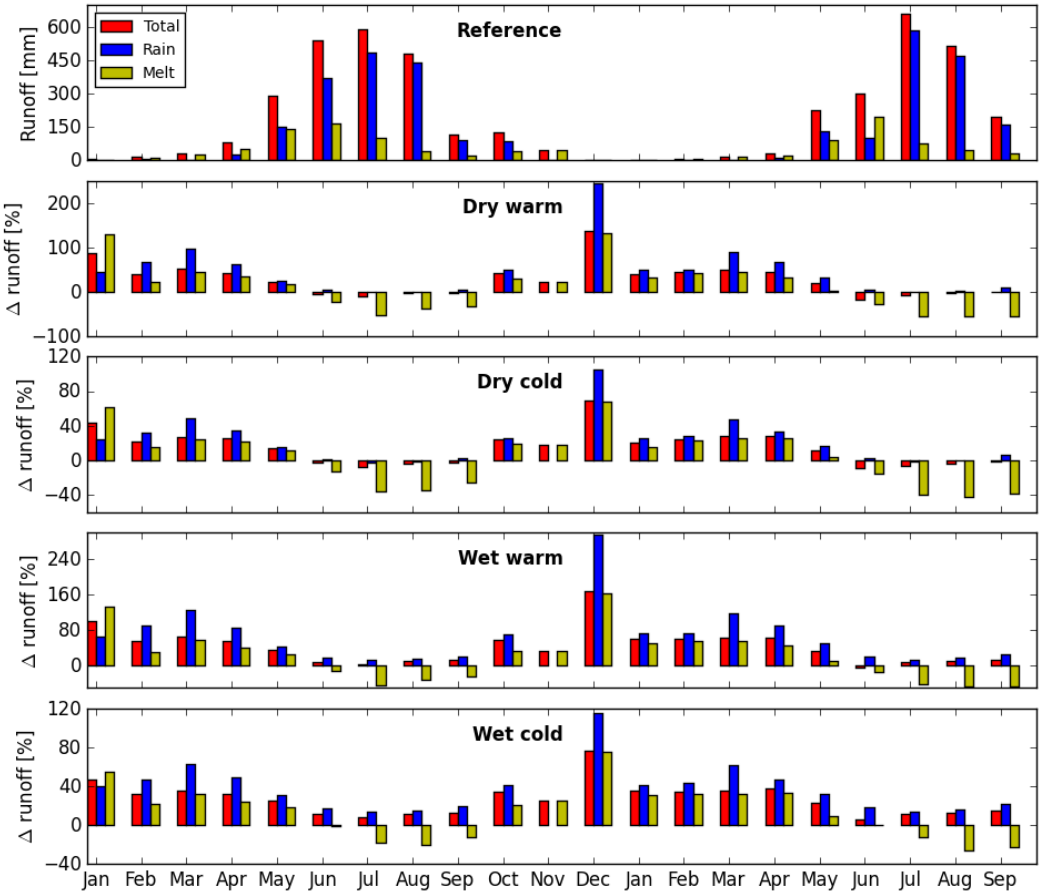
Reference
Total
Rain
Melt
Runoff [mm]
Dry warm
Dry cold
Wet warm
Wet cold
Δ runoff [%]
Jan Feb Mar Apr May Jun Jul Aug Sep Oct Nov Dec Jan Feb Mar Apr May Jun Jul Aug Sep

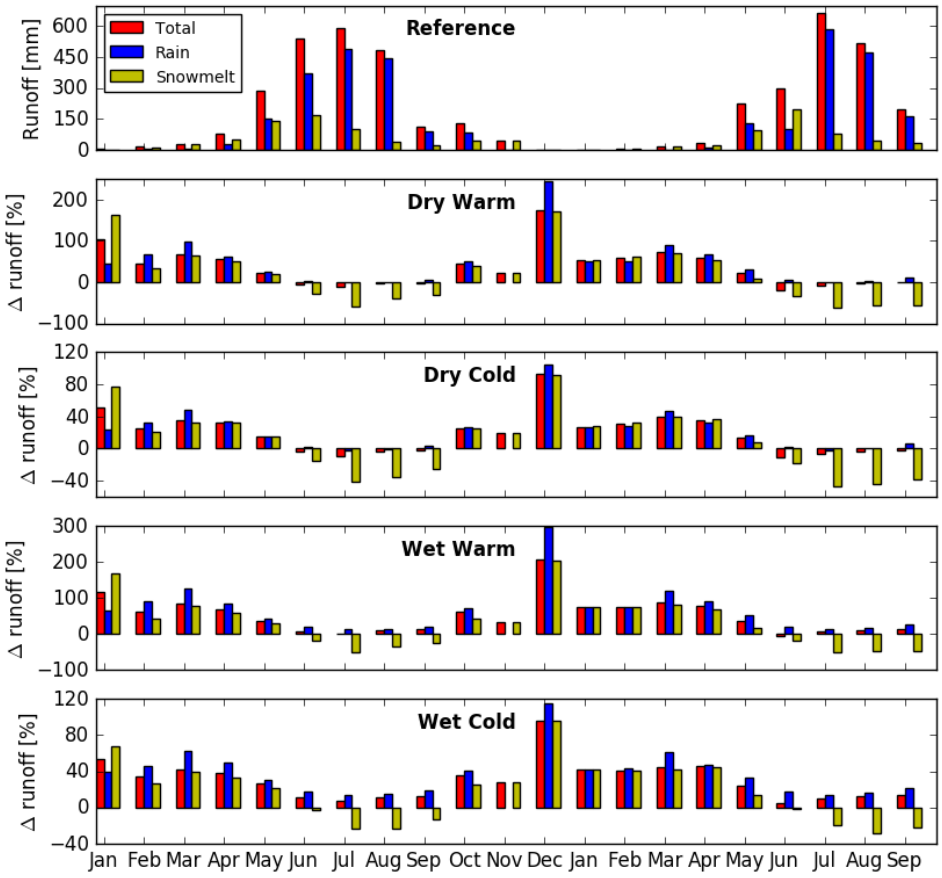

Figure 9: Modelled runoff at catchment outlet for the study period~~reference scenario~~ (January 2013 – September 2014) and change in runoff compared to the study period~~reference scenario~~ for the climate sensitivity tests.

Table 1: Overview of the in situ observations and their specifications. Locations are shown in Fig. 1.

Description	Code	Data availability	Latitude	Longitude	Elevation (m asl)	Observations[1]
Yala 1	Y1	06/05/13 – 03/05/14	28.22645	85.56878	4117	ST
Yala 2	Y2	06/05/13 – 03/05/14	28.22897	85.57391	4214	ST
Yala 3	Y3	06/05/13 – 03/05/14	28.2298	85.58051	4328	ST
Yala 4	Y4	06/05/13 – 02/03/14	28.22932	85.58492	4441	ST
Yala 5	Y5	06/05/13 – 03/05/14	28.22894	85.5908	4541	ST
Yala 6	Y6	06/05/13 – 03/05/14	28.22635	85.5918	4656	ST
Yala 7	Y7	06/05/13 – 02/03/14	28.22635	85.59246	4759	ST
Yala 8	Y8	06/05/13 – 02/03/14	28.23342	85.59921	4960	ST
Ganjala 1	G1	03/11/13 – 11/10/14	28.20305	85.56405	3908	ST
Ganjala 2	G2	03/11/13 – 06/09/14	28.20155	85.56577	3998	ST
Ganjala 3	G3	03/11/13 – 11/10/14	28.19899	85.56617	4094	ST
Ganjala 4	G4	03/11/13 – 30/04/14	28.1938	85.56916	4201	ST
Ganjala 5	G5	03/11/13 – 11/10/14	28.18831	85.57001	4300	ST
Pluvio Yala	Pluvio Y	01/01/13 – 30/06/13 26/10/13 – 16/10/14	28.22900	85.59700	4831	T, SD
Pluvio Ganjala	Pluvio G	20/01/14 – 03/05/14	28.18625	85.56961	4361	SD
Pluvio Langshisha	Pluvio L	29/10/13 – 01/07/14	28.20265	85.68619	4452	SD
Pluvio Morimoto	Pluvio M	17/05/13 – 09/10/14	28.25296	85.68152	4919	T, SD
Lama Hotel	T1	01/01/13 – 07/10/14	28.16212	85.43073	2492	T
Langtang	T2	01/01/13 – 07/10/14	28.21398	85.52745	3557	T
Jathang	T3	01/01/13 – 07/10/14	28.1958	85.6132	3947	T
Numthang	T4	01/01/13 – 07/10/14	28.20213	85.64313	3983	T
AWS Kyangjin	AWS K	01/01/13 – 07/10/14	28.2108	85.5695	3862	T, SD, P, IR
AWS_Yala_Base Camp	AWS Y	01/01/13 – 07/10/14	28.23252	85.61208	5090	SD

[1] ST, surface temperature; SD, snow depth; T, air temperature; P, precipitation; IR, incoming shortwave radiation

Table 2: Parameters in the snow model. Value indicates the uncalibrated parameter value and the value range indicates the range which is used for the sensitivity analysis. Sensitivity of snow depth (SD) and snow extent (SE) represent the difference between the 90th and 10th percentile of mean snow depth and snow extent resulting from the sensitivity analysis.

Para-meter	Unit	Description	Initial Value	Value range	Sensitivity SD [mm]	Sensitivity SE [km^2]
TT	[°C]	Threshold temperature for onset of melt or refreezing	0 [6]	-6 – 2 [4, 5, 6]	157.3	57.25
SRF	[m^2 mm W^{-2} d^{-1}]	Melt factor dependent on incoming shortwave radiation	0.15 [6]	0.13 – 0.19 [4, 6]	9.486	2.721
TF	[mm °C^{-1} d^{-1}]	Melt factor dependent on temperature	4.32 [6]	2.54 – 5.19 [4, 6]	9.486	2.721
thr_{snow}	[°C]	Threshold for partitioning in rain or snow	0 [6]	-1 – 1 [6,7]	35.82	11.99
C_{rf}	[mm °C^{-1} d^{-1}]	Degree-day refreezing factor	0.16 [7]	0.08 – 0.40 [7]	8.188	0.3248
a_{ini}	[-]	Decay of albedo deep snow (initial)	0.713 [2]	-	-	-
α_u	[-]	Albedo of surface underlying snow (ground, ice)	0.15, 0.25 [6]	-	-	-
a_1	[-]	Decay of albedo deep snow	0.112 [2]	0.112 – 0.34 [2,6]	56.39	7.279
a_2	[-]	Decay of albedo shallow snow	0.442 [2]	0.3 – 0.5	0.2410	0.2818
a_3	[-]	Decay of albedo shallow snow (exponent)	0.058 [2]	0.03 – 0.1	0.2001	0.2132
r_{max}	[-]	Maximum allowed fraction of liquid water in snowpack	0.1 [7]	0.05 – 0.20 [7]	31.66	0.3278
d^*	[cm]	Scaling length for smooth transition albedo from deep snow to shallow snow	2.4 [2]	1 – 25	0.0012	0.0007
SS_1	[m]	Regression function parameter snow holding depth dependence on slope angle	250 [6]	200 – 300	10.86	2.033
SS_2	[-]	Regression function parameter snow holding depth dependence on slope angle	0.172 [6]	0.16 – 0.19	26.45	7.170
S_{min}	[°]	Minimum slope for avalanching to occur	25 [1]	15 – 35	34.00	1.640
ρ_{av}	[kg L^{-1}]	Density of avalanching snow	0.200 [3]	-	-	-
ρ_{min}	[kg L^{-1}]	Minimum density of new snow due to snowfall	0.050 [7]	0.050 – 0.150 [7]		-
a_{ns}		Coefficient for density of new snow	100 [7]	-	-	-
η_0	[MN s m^{-2}]	Coefficient related to viscosity of snow (at zero temperature and density)	7.6 [7]	1 – 10 [7]	75.75	-
C_5	[°C^{-1}]	Coefficient for temperature effect on viscosity	0.1 [7]	0.04 – 0.12 [7]	10.44	-
C_6	[L kg^{-1}]	Coefficient for density effect on viscosity	21 [7]	15 – 35 [7]	268.8	-
k_{comp}	[-]	Compaction factor	0.5 [7]	-	-	-
precip	[-]	Precipitation correction factor	1	0.6 – 1.4	320.1	14.17
T_{lapse}	[-]	Temperature lapse rate correction factor	1	0.9 – 1.1	116.0	24.63

[1] Bernhardt and Schulz, 2010
[2] Brock et al., 2000
[3] Hopfinger, 1983
[4] Pellicciotti et al., 2012
[5] Ragettli et al., 2013
[6] Ragettli et al., 2015
[7] Saloranta, 2014

Table 3: Changes in temperature (ΔT) and precipitation (ΔP) for the climate sensitivity tests (same as Immerzeel et al. (2013)).

Sensitivity scenario	ΔT (°C)	ΔP (%)
Dry, cold	1.5	-3.2
Dry, warm	2.4	-2.3
Wet, cold	1.3	12.4
Wet, warm	2.4	12.1

Table 4: Confusion matrices for comparison of Landsat 8 snow maps and MOD10A2 snow maps with in situ snow observations.

		MOD10A2		Landsat 8	
		Snow	No snow	Snow	No Snow
In situ	Snow	83	31	20	3
	No Snow	75	438	18	106

Table 5: Confusion matrices for comparison of in situ snow observations provided by snow depth and surface temperature observations with remotely sensed snow maps (MOD10A2 and Landsat 8 combined).

		In situ snow depth		In situ surface temperature	
		Snow	No snow	Snow	No Snow
Remotely sensed	Snow	52	16	51	77
	No Snow	17	80	17	464

Table 6: Parameter value range prior to calibration and after calibration. The standard deviation of posterior parameter values is based on the standard deviation of all members.

Parameter	Prior (min-max)	Posterior mean	Posterior std.
TT	-6 – 2	-8.18	1.66
T_{lapse}	0.9 – 1.10	1.10	0.01
Precip	0.6 – 1.4	1.31	0.02
C_6	15 – 35	16.07	0.52

Table 7: Classification accuracy of modelled snow extent based on pixel comparison with Landsat 8 snow maps. Calibrated accuracies are averaged over all members and the standard deviation represents the standard deviation in individual member accuracies (after calibration).

Date	Accuracy uncalibrated (%)	Accuracy calibrated (%)	Std. dev. accuracy (%)
02/11/13	80.96	84.41	0.12
18/11/13	78.43	79.15	0.11
04/12/13	77.41	77.10	0.05
20/12/13	54.97	60.38	0.08
05/01/14	63.46	67.07	0.07
20/01/14	74.30	81.33	0.04
06/02/14	65.55	73.24	0.05
10/03/14	84.94	89.67	0.05
26/03/14	87.03	86.90	0.04
11/04/14	80.29	82.92	0.05